

A discussion of the reaction rate and the cell voltage of an intercalation electrode during discharge

Manuel Landstorfer

submitted: December 20, 2018

Weierstrass Institute
Mohrenstr. 39
10117 Berlin
Germany
E-Mail: manuel.landstorfer@wias-berlin.de

No. 2563
Berlin 2018



2010 *Mathematics Subject Classification.* 78A57, 35Q35, 34B15, 82B30, 82D25.

Key words and phrases. Butler–Volmer-equation, intercalation reaction, battery electrode, non-equilibrium thermodynamics, modeling, discharge simulation, cell voltage, parameter study.

The author acknowledges the financial support by the Federal Ministry of Education and Research of Germany (BMBF) in the framework mathematics for innovation (project number 05M18BCA).

Edited by
Weierstraß-Institut für Angewandte Analysis und Stochastik (WIAS)
Leibniz-Institut im Forschungsverbund Berlin e. V.
Mohrenstraße 39
10117 Berlin
Germany

Fax: +49 30 20372-303
E-Mail: preprint@wias-berlin.de
World Wide Web: <http://www.wias-berlin.de/>

A discussion of the reaction rate and the cell voltage of an intercalation electrode during discharge

Manuel Landstorfer

Abstract

In this work we discuss the modeling procedure and validation of a non-porous intercalation half-cell during galvanostatic discharge. The modeling is based on continuum thermodynamics with non-equilibrium processes in the active intercalation particle, the electrolyte, and the common interface where the intercalation reaction $\text{Li}^+ + \text{e}^- \rightleftharpoons \text{Li}$ occurs. This yields balance equations for the transport of charge and intercalated lithium in the intercalation compound, a surface reaction rate at the interface, and transport equations in the electrolyte for the concentration of lithium ions and the electrostatic potential. An expression for the measured cell voltage E is then rigorously derived for a half cell with metallic lithium as counter electrode. The model is then in detail investigated and discussed in terms of scalings of the non-equilibrium parameters, *i.e.* the diffusion coefficients D_A and D_E of the active phase and the electrolyte, conductivity σ_A and σ_E of both phases, and the exchange current density $e_0 L_s$, with numerical solutions of the underlying PDE system. The current density i as well as all non-equilibrium parameters are scaled with respect to the 1-C current density i_A^C of the intercalation electrode and the C-rate C_h of discharge. Further we derive an expression for the capacity Q of the intercalation cell, which allows us to compute numerically the cell voltage E as function of the capacity Q and the C-rate C_h . Within a hierarchy of approximations of the non-equilibrium processes we provide computations of $E(Q)$ for various values of the diffusion coefficients, the conductivities and the exchange current density. For the later we provide finally a discussion for possible concentration dependencies and (surface) thermodynamic consistency.

Contents

1	Introduction	2
2	Modeling	4
2.1	Material functions	6
2.2	Electroneutrality condition	7
2.3	Transport equations	8
2.4	Reaction rate based on surface thermodynamics	10
2.5	Cell Voltage	11
2.6	Current–Voltage relation	11
2.7	Onsager coefficient of the intercalation reaction	12
2.8	Discussion of the model parameters	13

3 Discussion	16
3.1 BV 0: Open circuit potential	17
3.2 BV 1: Infinite fast diffusion and conductivity in the active particle and the electrolyte	17
3.3 BV 2: Contribution of finite active phase conductivity	19
3.4 BV 3: Contribution of the solid-state diffusion in the active particle phase	20
3.5 BV 4: Finite conductivity in the electrolyte	23
3.6 BV 5: Finite diffusion in the electrolyte phase	24
4 Conclusion	29
4.1 Validation	29
4.2 Discussion of the exchange current density	30
4.3 Summary	34
Appendices	37
A Electrolyte	37
A.1 Mole fractions	37
A.2 Thermodynamic factor	37
A.3 PDEPE syntax for the electrolyte phase	38
B Active particle	40
B.1 Thermodynamic factor	40
B.2 PDEPE notation	40

1 Introduction

Lithium ion batteries (LIBs) are vital today for many branches of modern society and especially for electro-mobility. The German national platform electro-mobility aims one million electric vehicles by 2020, as well as the U.S., while China targets about five million zero emission cars. To achieve these goals, substantial knowledge on the effectively non-linear behavior of LIBs is required in order to reduce cost, increase their efficiency, safety, durability and further. The interpretation of experimental data requires a versatile and predictive mathematical model of a LIB, which accounts for the many physicochemical processes occurring simultaneously during charge and discharge, e.g. Li^+ diffusion in the electrolyte, surface reactions at the electrode/electrolyte interface, solid state diffusion in the active particles, and electrical conductivity.

First academic steps to model the functional principle of LIBs with the purpose of simulating their charge/discharge behavior were carried out by Newman *et al.* around 1993 [1]. This electrochemical model became a central tool to interpret measured data of intercalation batteries.

One of the central ingredients of the Newman model is the Butler–Volmer-type reaction rate R_s for the intercalation reaction $\text{Li}^+ + \text{e}^- \rightleftharpoons \text{Li}$ occurring at the interface $\Sigma_{\text{A,E}}$ between an intercalation electrode (particle) Ω_{A} and the electrolyte Ω_{E} . The actual functional dependency of $R_s = R_s(n_{\text{E}}, \varphi_{\text{E}}, n_{\text{A}}, \varphi_{\text{A}})$ on the different variables of the equation system, e.g. the electrolyte concentration n_{E} , the electrostatic potential φ_{E} in the electrolyte, the concentration n_{A} of intercalated ions, and the electrostatic potential φ_{A} of the active phase, is, however, rather stated than derived. Especially the so called exchange current density and its functional relationship to the cation concentration is doubtful.

From a non-equilibrium thermodynamics (NET) point of view, the functional dependency $R_s = R_s(n_{\text{E}}, \varphi_{\text{E}}, n_{\text{A}}, \varphi_{\text{A}})$ can be consistently derived and NET restricts this functional dependency in a very specific manner. We discuss in this work the modeling procedure of a single transfer reaction at the interface between an active intercalation phase and some electrolyte based on the framework of NET for volumes and surfaces and draw some conclusions regarding thermodynamic consistent models of the reaction rate. We account also for diffusion processes in the adjacent active particle and the electrolyte, as well as electrical conductivity, and state the corresponding balance equations. Then we consider galvanostatic discharge in half cell of some cathode intercalation material, electrolyte, and a lithium reference electrode, which is considered as ideally polarizable counter electrode.

We introduce the C_1 -current density, *i.e.* the current at which the electrode is completely discharged during one hour, and scale all non-equilibrium parameters based on the C -rate C_h , *i.e.* multiples of the C_1 current density. It is then possible to derive a general relation between the measured cell voltage E , the capacity Q , and the C -rate C_h based on the reaction rate $R_s = R_s(n_{\text{E}}, \varphi_{\text{E}}, n_{\text{A}}, \varphi_{\text{A}})$. Since, however, actually the concentrations at the interface $\Sigma_{\text{A,E}}$ of intercalated cations n_{A} and electrolytic cations n_{E} enter the surface reaction rate R_s , we need to solve necessarily the diffusion equations in the adjacent phases. We discuss various approximation regimes and parameter scalings of the non-equilibrium parameters which allows us to compare numerical simulations of cell voltage $E = E(Q, C_h)$ to some representative experimental examples, especially of $\text{Li}_x(\text{Ni}_{1/3}\text{Mn}_{1/3}\text{Co}_{1/3}\text{O}_2)$ (NMC). Fig. shows the measured cell voltage E as function of the capacity (or status of charge) for various discharge rates of thin of NMC half cell [2].

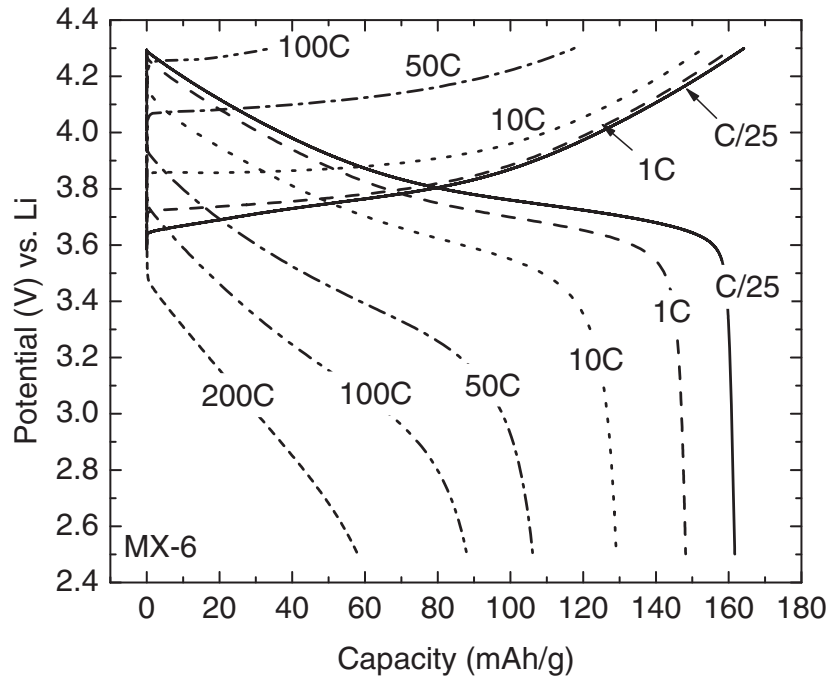


Figure 1: Discharge curves (lower part) for various C-rates (Data of Fig 1.b from [2] , reprinted with permission of The Electrochemical Society)

We show that a rather *simple* (but thermodynamically consistent) model of the surface reaction rate R_s , or more precise of the exchange current density, is sufficient to understand and predict the complex non-linear behavior of the cell voltage as function of the capacity Q and the C-Rate C_h . We provide also computations of $E = E(Q, C_h)$ for the exchange current density introduced by *Newman et. al*, draw some regarding thermodynamic consistency, and compare computations based on this expression to the cell voltage based on our *simple* expression of the current density.

2 Modeling

We consider an active intercalation particle Ω_A in contact with some electrolyte Ω_E . The interface $\Sigma_{A,E} = \Omega_A \cap \Omega_E$ captures the actual surface Σ_A of the active particle as well as the electrochemical double layer forming at the interface, *i.e.* $\Sigma_{A,E} = \Omega_A^{\text{SCL}} \cup \Sigma_A \cup \Omega_E^{\text{SCL}}$. The domains Ω_E and Ω_A are thus electro-neutral, and we refer to [3–5] for details on the derivation. The electrolyte is on the right side in contact to some metallic counter electrode Ω_C , where at the interface $\Sigma_{E,C}$ captures also the double layer forming at the interface between the electrolyte and the counter electrode Ω_C .

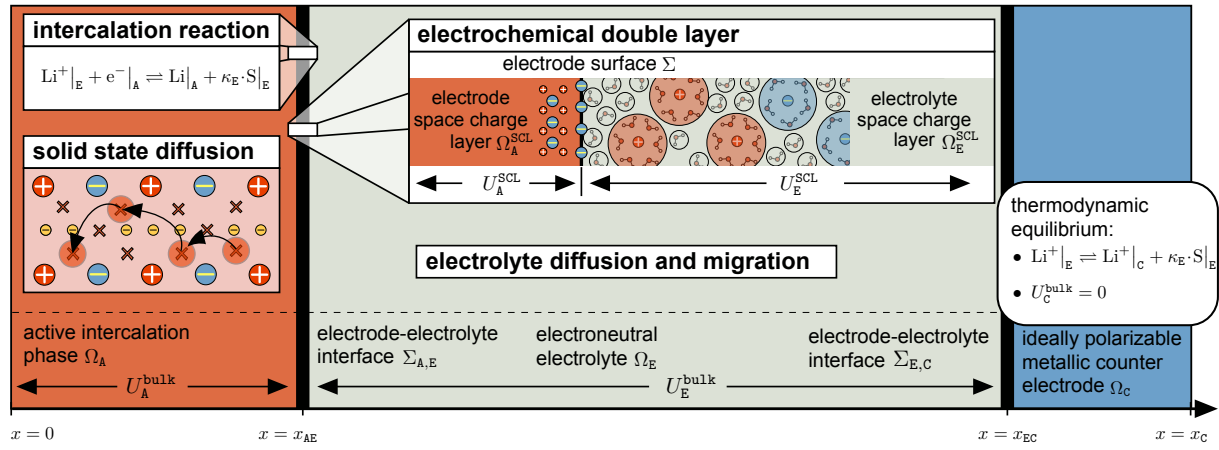


Figure 2: Sketch of an active intercalation phase Ω_A in contact with some electrolyte Ω_E . The electrode-electrolyte interface $\Sigma_{A,E}$ covers the space charge layer Ω_E^{SCL} of the electrolyte and Ω_A^{SCL} of the electrode as well as the actual electrode surface Σ . Several processes occur simultaneously, *i.e.* the intercalation reaction, electrolyte diffusion and solid state diffusion as well as electrical conductivity.

We consider a 1D approximation, where the electrode-electrolyte interface $\Sigma_{A,E}$ is positioned at $x = x_{AE}$, the left boundary of Ω_A is denoted by $x = 0$ and the right boundary of Ω_E is $x = x_{EC}$, with $d_A = |x_{AE}|$ and $d_E = |x_{EC} - x_{AE}|$. The counter electrode is positioned at $x = x_{EC}$ and spans to $x = x_C$.

For some quantity $u(x, t)$, we denote with

$$u|_{AE}^{\pm} = u|_{x=x_{AE}}^{\mp} \quad \text{and} \quad u|_{EC}^{\pm} = u|_{x=x_{EC}}^{\mp} \quad (1)$$

the evaluation at the respective side of the interface $\Sigma_{A,E}$ and $\Sigma_{E,C}$, respectively. If u is present only on one phase, we drop the superscript \pm .

The active particle Ω_A is a mixture of electrons e^- , intercalated cations C and lattice ions M^+ , and the electrolyte a mixture of solvated cations C^+ , solvated anions A^- and solvent molecules S . The respective species densities are denoted with $n_\alpha(\mathbf{x}, t)$, $\mathbf{x} \in \Omega_i$. We denote with

$$\mu_\alpha = \frac{\partial \psi}{\partial n_\alpha} \quad , \quad i = A, E, \quad \alpha = E_A, E_C, E_S, A_C, A_e, A_M \quad , \quad (2)$$

the chemical potential of the constituents, which are derived from a free energy density [6, 7] $\psi = \psi_A + \psi_E$ with $\psi_A = \hat{\psi}_A(n_{A_e}, n_{A_C}, n_{A_M})$ of the active particle and $\psi_E = \hat{\psi}_E(n_{E_S}, n_{E_A}, n_{E_C})$ of the electrolyte phase.

For the surface Σ we have surface chemical potentials [4, 6, 8, 9]

$$\mu_\alpha^s = \frac{\partial \psi_s}{\partial n_\alpha^s} \quad , \quad \alpha = E_A, E_C, E_S, A_C, A_e, A_M \quad , \quad (3)$$

which are derived from some general surface free energy density ψ_s .

2.1 Material functions

For the electrolyte we consider exclusively the material model [9–11] of an incompressible liquid electrolyte accounting for solvation effects, *i.e.*

$$\mu_\alpha = g_\alpha^R + k_B T \ln(y_\alpha) + v_\alpha^R(p - p^R) \quad \alpha = E_S, E_A, E_C, \quad (4)$$

with mole fraction

$$y_\alpha = \frac{n_\alpha}{n_E^{\text{tot}}}, \quad (5)$$

molar concentration n_α , and total molar concentration of the mixture (with respect to the number of mixing particles [9])

$$n_E^{\text{tot}} = n_{E_S} + n_{E_A} + n_{E_C}. \quad (6)$$

Note that n_{E_S} denotes the number of *free* solvent molecules, whereas n_{E_A} and n_{E_C} are the densities of the solvated ions. This is crucial for various aspects of the thermodynamic model, and we refer to [9, 10, 12, 13] for details. Overall, the material model for the electrolyte corresponds to an incompressible mixture with solvation effects. We assume further

$$\frac{v_{E_C}^R}{v_{E_S}^R} = \frac{m_{E_C}}{m_{E_S}} \quad \text{and} \quad \frac{v_{E_A}^R}{v_{E_S}^R} = \frac{m_{E_A}}{m_{E_S}} \quad (7)$$

whereby the incompressibility constraint [9–11] implies also a conservation of mass, *i.e.*

$$\sum_\alpha v_\alpha^R n_\alpha = 1 \quad \Leftrightarrow \quad \sum_\alpha m_\alpha n_\alpha = \rho = \frac{m_{E_S}}{v_{E_S}^R} = \text{const.} \quad (8)$$

The molar volume of the solvent is related to the mole density $n_{E_S}^R$ of the pure solvent as

$$v_{E_S}^R = (n_{E_S}^R)^{-1}. \quad (9)$$

Note further that the partial molar volumes v_α^R and the molar masses m_α of the cation and anion are related to the solvation number κ_E and κ_{A_C} , respectively.

We assume that partial molar volume of the ionic species is mainly determined by the solvation shell, which seems reasonable for large solvents like DMC in comparison to the small ions like Li^+ . We proceed thus with the assumption

$$v_{E_C} = \kappa_E \cdot v_{E_S} \quad \text{and} \quad v_{E_A} = \kappa_E \cdot v_{A_C}. \quad (10)$$

For the active particle, we consider an extension of a classical lattice mixture model [14–21] which accounts for occupation numbers $\omega_A > 1$ as well as a Redlich–Kister type enthalpy term [22, 23] for the intercalation material $\text{Li}_y(\text{Ni}_{1/3}\text{Mn}_{1/3}\text{Co}_{1/3})\text{O}_2$ (NMC). We refer to [24] for a detailed discussion and derivation based on a free energy ψ^A . The chemical potential of intercalated lithium is derived as

$$\mu_{A_C} = k_B T \left(\ln \left(\frac{\frac{1}{\omega_A} y_{A_C}}{1 + \frac{1-\omega_A}{\omega_A} y_{A_C}} \right) - \omega_A \cdot \ln \left(\frac{1 - y_{A_C}}{1 + \frac{1-\omega_A}{\omega_A} y_{A_C}} \right) + \gamma_A \cdot g_A(y_{A_C}) \right) \quad (11)$$

with

$$g(y) = (2y-1) + \frac{1}{2}(6y(1-y) - 1) - \frac{1}{3}(8y(1-y) - 1)(2y-1) \quad (12)$$

and mole fraction

$$y_{AC} = \frac{n_{AC}}{n_{A\ell}} \quad (13)$$

of intercalated cations in the active phase. The number density $n_{A\ell}$ of lattice sites is constant, which corresponds to an incompressible lattice, and the enthalpy parameter $\gamma_A < 2.5$. Note that $\gamma_A > 2.5$ entails a phase separation [20] and requires an additional term $\gamma_A \text{div} \nabla y_{AC}$ in the chemical potential. However, we assume throughout this work that no phase separation occurs, whereby in diffusional equilibrium of the intercalation phase the concentration is homogeneous. An extension of this discussion towards phase separating materials will be given in a subsequent work.

For the electrons we consider [9, 25]

$$\mu_{Ae} = \left(\frac{3}{8\pi}\right)^{\frac{2}{3}} \frac{\hbar^2}{2m_{Ae}} n_{Ae}^{\frac{2}{3}} \quad \text{and} \quad \mu_{Ae}^R = g_{Ae}^R = \text{const.} \quad (14)$$

and for the lattice ions

$$\mu_{AM} = g_{AM}^R + k_B T \ln(1 - y_{AC}) + v_M^R (p_M - p_M^R), \quad (15)$$

where $v_M^R = (n_M^R)^{-1}$ is the molar volume of the lattice ions, p_M the partial pressure and g_{AM}^R the constant molar Gibbs energy. The material functions of the active intercalation electrode essentially model an incompressible solid with a sub-lattice for the intercalated cations A_C .

The explicit surface chemical potentials

$$\mu_{\alpha}^s = \frac{\partial \psi}{\partial n_{\alpha}^s}, \quad \alpha = E_A, E_C, E_S, A_C, A_M, \quad (16)$$

are not required throughout this work since we will assume that the double layer is in equilibrium and that the double layer capacity (and thus also adsorption), is negligible for the sake of this work. However, we refer to [9] for the explicit functions of μ_{α}^s and the surface free energy of a surface lattice mixture with solvation effects.

2.2 Electroneutrality condition

The electroneutrality condition of Ω_A , Ω_E and Ω_C can be obtained by an asymptotic expansion of the balance equations in the electrochemical double layer at the respective surface Σ . We only briefly recapture the central conclusions and refer to [3–5, 9, 26] for details on the modeling, validation and the asymptotics. Most importantly, we have that

- the double layer is in thermodynamic equilibrium, *i.e.* $\nabla \mu_{\alpha} + e_0 z_{\alpha} \nabla \varphi = 0$ in Ω_A^{SCL} and Ω_E^{SCL}

- there exists a potential drop between the active particle surface Σ and the hyper-surface $\Sigma_{A,E}^\pm$ outside of the respective space charge layers which is denoted by

$$U_i^{\text{SCL}} = \varphi - \varphi|_s^i, \quad i = A, E \quad (17)$$

where $\varphi|_s^i$ is the electrostatic potential *right outside* the space charge layer in the electrolyte or the active particle, respectively, and φ the (continuous) potential at the surface Σ ¹. The whole potential drop across the double layer at $\Sigma_{A,E}$ is denoted by

$$U_{AE}^{\text{DL}} = U_E^{\text{SCL}} - U_A^{\text{SCL}} = \varphi|_{AE}^+ - \varphi|_{AE}^- \quad (18)$$

- the chemical potential at the surface can be *pulled back* through the double layer, *i.e.* $\mu_\alpha = \mu_\alpha^i - e_0 z_\alpha U_i^{\text{SCL}}$, $i = A, E$
- the condition $\mu_e = \text{const.}$ entails that the potential drop U_A^{SCL} is constant (with respect to some applied voltage) and determined by

$$U_A^{\text{SCL}} = \frac{1}{e_0} (\mu_{Ae} - \mu_{Ae}|_{AE}). \quad (19)$$

- and that for monovalent electrolytes the cation mole fraction (or number density) is equal to the anion mole fraction, *i.e.*

$$y_{EC} = y_{AC}. \quad (20)$$

- in the active phase the electroneutrality entails

$$n_{Ae} = n_{AM} = \text{const.} \quad (21)$$

whereby we abbreviate

$$g_{Ae}^R := \mu_{Ae}(n_{AM}) \quad (22)$$

which is basically the Fermi energy of the solid material.

2.3 Transport equations

In the electrolyte Ω_E we have two balance equations determining the concentration $n_{EC}(x, t)$ (or mole fraction $y_{EC}(x, t)$) and the electrostatic potential $\varphi_E(x, t)$ in the electrolyte [27–32], *i.e.*

$$\frac{\partial n_{EC}}{\partial t} = -\partial_x J_{EC} \quad \text{with} \quad J_{EC} = -D_E \cdot n_E^{\text{tot}} \Gamma_E^{\text{tf}} \cdot \partial_x y_{EC} + \frac{t_{EC}}{e_0} J_{E,q} \quad (23)$$

$$0 = -\partial_x J_{E,q} \quad \text{with} \quad J_{E,q} = -S_E \cdot n_E^{\text{tot}} \Gamma_E^{\text{tf}} \partial_x y_E - \Lambda_E n_E \partial_x \varphi_E \quad (24)$$

with (dimensionless) thermodynamic factor

$$\Gamma_E^{\text{tf}} = \frac{y_{EC}}{k_B T} \frac{\partial \hat{\mu}_{EC}}{\partial y_{EC}} = 1 + 2\kappa_E \frac{y_E}{1 - 2y_{EC}} = \Gamma_E^{\text{tf}}(y_E). \quad (25)$$

¹Note that the continuity of φ across Σ is an assumption.

where

$$\hat{\mu}_{\text{E}_C} = \mu_{\text{E}_C} - \frac{m_{\text{E}_C}}{m_{\text{E}_S}} \mu_{\text{E}_S} = k_{\text{B}} T (\ln(y_{\text{E}_C}) - \kappa_{\text{E}} \ln(y_{\text{E}_S})) \quad (26)$$

is the thermodynamic driving force for diffusion [11]. Note that we assumed $\frac{v_{\text{E}_C}^R}{v_{\text{E}_S}^R} = \frac{m_{\text{E}_C}}{m_{\text{E}_S}}$ and $v_{\text{E}_C}^R = \kappa_{\text{E}} \cdot v_{\text{E}_S}^R$ which yields the representation (26). Note further that the total number density $n_{\text{E}}^{\text{tot}} = n_{\text{E}_S} + n_{\text{E}_C} + n_{\text{E}_A}$ in the electrolyte writes as

$$n_{\text{E}}^{\text{tot}} = n_{\text{E}_S}^R \cdot \frac{1}{1 + 2(\kappa_{\text{E}} - 1)y_{\text{E}}} = n_{\text{E}}^{\text{tot}}(y_{\text{E}}) \quad (27)$$

which is determined from the incompressibility constraint (8)

$$v_{\text{E}_S}^R n_{\text{E}_S} + v_{\text{E}_A}^R n_{\text{E}_A} + v_{\text{E}_C}^R n_{\text{E}_C} = 1 \quad (28)$$

and the electrolyte concentration n_{E_C} in terms of y_{E_C} as

$$n_{\text{E}_C} = y_{\text{E}_C} \cdot n = n_{\text{E}_S}^R \frac{y_{\text{E}_C}}{1 + 2(\kappa_{\text{E}} - 1)y_{\text{E}}} = n_{\text{E}_C}(y_{\text{E}}). \quad (29)$$

If we consider a simple Nernst–Planck–flux relation for the cation and anion fluxes [11, 33], respectively, *i.e.*

$$\mathbf{J}_{\alpha} = D_{\alpha}^{\text{NP}} \frac{n_{\alpha}}{k_{\text{B}} T} (\nabla \mu_{\alpha} - \frac{m_{\alpha}}{m_0} \nabla \mu_{\text{E}_S} + e_0 z_{\alpha} n_{\alpha} \nabla \varphi_{\text{E}}) \quad \alpha = \text{E}_A, \text{E}_C, \quad (30)$$

with constant diffusion coefficients $D_{\text{E}_A}^{\text{NP}}$ for the anion and $D_{\text{E}_C}^{\text{NP}}$ for the cation, we obtain (in the electroneutral electrolyte)

$$D_{\text{E}} = \frac{2D_{\text{E}_C}^{\text{NP}} \cdot D_{\text{E}_A}^{\text{NP}}}{D_{\text{E}_A}^{\text{NP}} + D_{\text{E}_C}^{\text{NP}}} \quad t_{\text{E}_C} = \frac{D_{\text{E}_C}^{\text{NP}}}{D_{\text{E}_A}^{\text{NP}} + D_{\text{E}_C}^{\text{NP}}} \quad (31)$$

$$\Lambda_{\text{E}} = \frac{e_0^2}{k_{\text{B}} T} (D_{\text{E}_A}^{\text{NP}} + D_{\text{E}_C}^{\text{NP}}) \quad S = e_0 (D_{\text{E}_C}^{\text{NP}} - D_{\text{E}_A}^{\text{NP}}) \quad (32)$$

Note, however, for general Maxwell–Stefan type diffusion [29–32, 34] or cross-diffusion coefficients [7, 24, 35] in the cation and anion fluxes lead to more *complex* representations of the transport parameters (t_{E_C} , S_{E} , D_{E} , Λ_{E}). In general, three of the transport parameters are *independent*, and S_{E} , t_{E_C} and Λ_{E} are related to each other via

$$\frac{k_{\text{B}} T}{e_0} (2t_{\text{E}_C} - 1) = \frac{S_{\text{E}}}{\Lambda_{\text{E}}}. \quad (33)$$

Further, (t_{E_C} , S_{E} , D_{E} , Λ_{E}) depend in general non-linearly on the electrolyte concentration n_{E_C} . However, it is sufficient for the sake of this work to assume constant values for the transport parameters (t_{E_C} , S_{E} , D_{E} , Λ_{E}), together with relation (33).

In the active particle Ω_{A} we have two balance equations determining the concentration $n_{\text{A}_C}(x, t)$ (or mole fraction y_{A_C}) and the electrostatic potential $\varphi_{\text{A}}(x, t)$ in the active particle, *i.e.*

$$\frac{\partial n_{\text{A}_C}}{\partial t} = -\partial_x J_{\text{A}_C} \quad \text{with} \quad J_{\text{A}_C} = -D_{\text{A}} \cdot n_{\text{A}_\ell} \Gamma_{\text{A}}^{\text{tf}} \cdot \partial_x y_{\text{A}_C} \quad (34)$$

$$0 = -\partial_x J_{\text{A},q} \quad \text{with} \quad J_{\text{A},q} = -\sigma_{\text{A}} \partial_x \varphi_{\text{A}} \quad (35)$$

and (dimensionless) thermodynamic factor

$$\Gamma_{\text{A}}^{\text{tf}} = \frac{y_{\text{A}}}{k_{\text{B}} T} \frac{\partial \mu_{\text{A}}}{\partial y_{\text{A}}} = 1 + \frac{y_{\text{A}}}{1 - y_{\text{A}}} - 2\gamma_{\text{A}} y_{\text{A}} = \Gamma_{\text{A}}^{\text{tf}}(y_{\text{A}}). \quad (36)$$

Note that in principle σ_{A} can be dependent on the amount of intercalated ions, *i.e.* $\sigma_{\text{A}} = \sigma_{\text{A}}(y_{\text{A}})$.

2.4 Reaction rate based on surface thermodynamics

We want to investigate the non-equilibrium thermodynamic modeling of the intercalation reaction



Surface thermodynamics dictates that the reaction rate R_s of this process can in general be written as [4, 5, 13, 36, 37]

$$R_s = L_s \cdot \left(e^{\alpha \cdot \frac{1}{k_{\text{B}}T} \lambda} - e^{-(1-\alpha) \cdot \frac{1}{k_{\text{B}}T} \lambda} \right) \quad \text{with} \quad \lambda_s = \mu_{\text{A}_C} + \kappa_{\text{E}} \cdot \mu_{\text{E}_S} - \mu_{\text{E}_C} - \mu_{\text{A}_e} , \quad (38)$$

with $\alpha \in [0, 1]$. Note that a non-negative function L_s in (38) ensures a non-negative entropy production $r_{\sigma,R}$ due to reactions on the surface, *i.e.* $r_{\sigma,R} = \lambda \cdot R_s > 0$.

The quantity λ_s can be considered as surface affinity of the reaction (37). The surface reaction rate R_s vanishes when the affinity vanishes, which is the actually the thermodynamic equilibrium condition of (37), *i.e.* $\lambda = 0 \Leftrightarrow r_{\sigma,R} = 0$.

Since the electrochemical double layer is in equilibrium, we can *pull back* the surface chemical potentials μ_{α} through the double layer to the respective *points* (in an asymptotic sense) outside of the double layer, whereby we obtain for the surface affinity

$$\lambda_s = \mu_{\text{A}_C} \Big|_{\text{AE}}^- + \kappa_{\text{E}} \cdot \mu_{\text{E}_S} \Big|_{\text{AE}}^+ - \mu_{\text{E}_C} \Big|_{\text{AE}}^+ + e_0 U_{\text{A,E}}^{\text{DL}} - \mu_{\text{A}_e} \Big|_{\text{AE}}^- . \quad (39)$$

With the material models (4) and (11) we can rewrite the surface affinity as

$$\lambda_s = e_0 (U_{\text{A,E}}^{\text{DL}} - E_{\text{A,E}}^T) + k_{\text{B}}T \left(f_{\text{A}}(y_{\text{A}_C} |_{\text{AE}}) - f_{\text{E}}(y_{\text{E}_C} |_{\text{AE}}) \right) \quad (40)$$

with

$$E_{\text{A,E}}^T := \frac{1}{e_0} (g_{\text{E}_C}^R + g_{\text{A}_e}^R - g_{\text{A}_C}^R - \kappa_{\text{E}} g_{\text{E}_S}^R) \quad (41)$$

and

$$f_{\text{E}}(y_{\text{E}_C}) := \ln \left(\frac{y_{\text{E}_C}}{\left(\hat{y}_{\text{E}_S}(y_{\text{E}_C}) \right)^{\kappa_{\text{E}}}} \right) , \quad (42)$$

$$f_{\text{A}}(y_{\text{A}_C}) := \ln \left(\frac{\frac{1}{\omega_{\text{A}}} y_{\text{A}_C}}{1 + \frac{1-\omega_{\text{A}}}{\omega_{\text{A}}} y_{\text{A}_C}} \right) - \omega_{\text{A}} \cdot \ln \left(\frac{1 - y_{\text{A}_C}}{1 + \frac{1-\omega_{\text{A}}}{\omega_{\text{A}}} y_{\text{A}_C}} \right) + \gamma_{\text{A}} \cdot g_{\text{A}}(y_{\text{A}_C}) \quad (43)$$

with g_{A} according to (12). Note again that $y_{\text{A}_C} |_{\text{AE}}$ denotes the evaluation of y_{A_C} at the interface $\Sigma_{\text{A,E}}$ and that the surface affinity (40) is dependent on the chemical potential (or the mole fraction) evaluated at the interface.

2.5 Cell Voltage

We consider the cell voltage in a half cell with metallic lithium as counter electrode, denoted by C and position at $x = x_{\text{EC}}$ (see Fig. 2). The cell voltage in such a cell is

$$E = \underbrace{\varphi|_{x=0} - \varphi|_{\text{AE}}^+}_{:= -U_{\text{A}}^{\text{bulk}}} + \underbrace{\varphi|_{\text{AE}}^+ - \varphi|_{\text{AE}}^-}_{= U_{\text{AE}}^{\text{DL}}} + \underbrace{\varphi|_{\text{AE}}^+ - \varphi|_{\text{EC}}^-}_{:= U_{\text{E}}^{\text{bulk}}} + \underbrace{\varphi|_{\text{EC}}^- - \varphi|_{\text{EC}}^+}_{U_{\text{EC}}^{\text{DL}}} + \underbrace{\varphi|_{x=x_{\text{EC}}}^+ - \varphi|_{x=x_{\text{C}}}}_{:= U_{\text{C}}^{\text{bulk}}}, \quad (44)$$

where $U_{\text{A}}^{\text{bulk}}$ is the potential drop in the bulk active particle due to the electron transport, $U_{\text{A,E}}^{\text{DL}}$ is the potential drop across the double layer at the interface between the active particle and the electrolyte, and $U_{\text{E}}^{\text{bulk}}$ the bulk potential drop due to cation electric current.

We assume that the counter electrode Ω_{C} is *ideally polarizable* [28], whereby the reaction



at the the interface $\Sigma_{\text{E,C}}$ positioned at $x = x_{\text{EC}}$ is in thermodynamic equilibrium and $U_{\text{C}}^{\text{bulk}} = \varphi|_{x=x_{\text{EC}}}^- - \varphi|_{x=x_{\text{C}}} = 0$. The equilibrium condition of (45) entails

$$U_{\text{EC}}^{\text{DL}} = \varphi|_{x=x_{\text{EC}}}^- - \varphi|_{x=x_{\text{EC}}}^+ = \frac{1}{e_0} \left(\mu_{\text{C}_\text{C}} - \mu_{\text{E}_\text{C}}|_{\text{EC}}^- + \kappa_{\text{E}} \mu_{\text{E}_\text{S}}|_{\text{EC}}^- \right) \quad (46)$$

$$= \frac{1}{e_0} (\mu_{\text{C}_\text{C}} - g_{\text{A}_\text{C}}^{\text{R}} - \kappa_{\text{E}} g_{\text{E}_\text{S}}^{\text{R}}) - \frac{k_{\text{B}} T}{e_0} f_{\text{E}}(y_{\text{E}_\text{C}}|_{\text{EC}}) \quad (47)$$

where $\mu_{\text{C}_\text{C}} = \text{const.}$ is the chemical potential of the metallic lithium.

For the surface affinity (40) we obtain the compact typeface

$$\lambda_s = e_0 (E + U_{\text{A}}^{\text{bulk}} - U_{\text{E}}^{\text{bulk}} - E_{\text{A,C}}) + k_{\text{B}} T (f_{\text{A}} - f_{\text{E}}|_{\text{AE}} + f_{\text{E}}|_{\text{EC}}) \quad (48)$$

with

$$E_{\text{A,C}} = \frac{1}{e_0} (\mu_{\text{C}_\text{C}} - g_{\text{A}_\text{C}}^{\text{R}} + g_{\text{A}_\text{e}}^{\text{R}}). \quad (49)$$

and

$$f_{\text{E}}|_{\text{AE}} = f_{\text{E}}(y_{\text{E}_\text{C}}|_{\text{AE}}) \quad \text{and} \quad f_{\text{E}}|_{\text{EC}} = f_{\text{E}}(y_{\text{E}_\text{C}}|_{\text{EC}}). \quad (50)$$

2.6 Current–Voltage relation

For the single intercalation reaction we have the following expression [4]

$$i = -e_0 R_s + C_{\text{E}}^{\text{DL}} \cdot \frac{dU_{\text{E}}^{\text{SCL}}}{dt} \quad (51)$$

for the current density i flowing out of the electrode Ω_{A} , where C_{E}^{DL} is the double layer capacity.

Note that the reaction rate is

$$R_s = L_s \cdot g\left(\frac{1}{k_{\text{B}} T_s} \lambda\right) \quad \text{with} \quad g(x) = \left(e^{\alpha x} - e^{-(1-\alpha)x} \right). \quad (52)$$

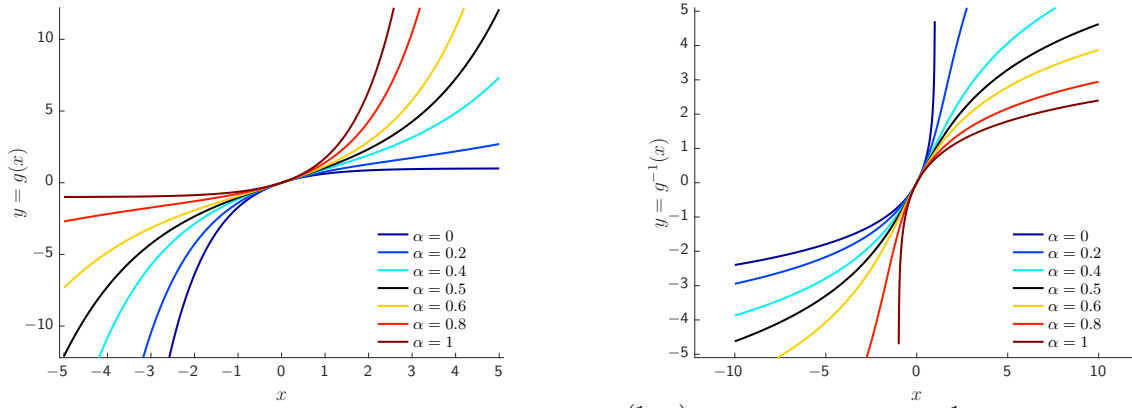


Figure 3: Reaction rate function $g(x) = e^{\alpha \cdot x} - e^{-(1-\alpha) \cdot x}$ and its inverse g^{-1} for various values of α .

Since $g(x)$ is a strictly monotone function, we can introduce the inverse of g , i.e. g^{-1} . For $\alpha = \frac{1}{2}$ we have $g(x) = 2\sinh\left(\frac{1}{2}x\right)$ and $g^{-1}(y) = 2g^{-1}\left(\frac{1}{2}y\right)$. For values $\alpha \neq 0.5$ the inverse function g^{-1} is only implicitly given, however, can easily be calculated numerically. Fig. displays the functions g and g^{-1} for various values of α . We call $g(x)$ the reaction rate function and g^{-1} the inverse reaction rate function.

Note that in the Tafel approximation $g\left(\frac{1}{k_B T} \lambda\right) \approx \frac{1}{k_B T} \lambda$ eq. (51) yields²

$$\frac{e_0}{k_B T} U_E^{\text{DL}} - \frac{1}{e_0 L_s} C_E^{\text{DL}} \cdot \frac{dU_E^{\text{DL}}}{dt} = \frac{e_0}{k_B T} E_{A,E}^T - (f_A - f_E) - \frac{1}{e_0 L_s} i \quad (53)$$

The term $e_0 L_s$ can be considered as the *exchange current density* [28].

2.7 Onsager coefficient of the intercalation reaction

The Onsager coefficient L_s (or the exchange current density $e_0 L_s$) of the surface reaction (37) could in principle be a function of the surface chemical potentials (or surface concentrations), i.e. $L_s = L_s(\mu_{A_C}, \mu_{E_C}, \mu_{E_S}, \mu_{A_e})$ or $L_s = L_s(\lambda)$ or the surface affinity, i.e. $L_s = L_s(\lambda)$, as long as the condition $L_s > 0$ is ensured [4, 8, 26]. Note, however, that surface thermodynamics dictates the dependency of L_s on the surface chemical potentials μ_α and not the bulk chemical potentials μ_α .

For a general relation $L_s = L_s(\mu_{A_C}, \mu_{E_C}, \mu_{E_S})$ we can *pull back* the surface chemical potentials μ_α through the double layer to obtain

$$L_s = L_s\left(\mu_{A_C}(y_{A_C}|_{AE}), \mu_{E_C}(y_{E_C}|_{AE}^+), -e_0 U_E^{\text{SCL}}, \mu_{E_S}(y_{E_S}|_{AE}^+)\right). \quad (54)$$

Note that this necessarily restricts the functional dependency of L_s on the mole fractions $y_\alpha|_{A,E}$ at the interface $\Sigma_{A,E}$.

²Note again that $U_{AE}^{\text{DL}} = U_E^{\text{SCL}} - U_A^{\text{SCL}}$ and that the space charge layer drop U_A^{SCL} is constant due to the material model $\mu_{A_e} = \text{const.}$ whereby $\frac{dU_E^{\text{SCL}}}{dt} = \frac{dU_{AE}^{\text{DL}}}{dt}$.

Consider, for example a model $L_s = L_s^E(y_{EC}|_{AE}^+)$, where the exchange current density is dependent on the electrolyte concentration at the interface. This would be, however, thermodynamically inconsistent since the general functional dependency of (54) requires for the electrolyte concentration at the interface

$$L_s = L_s^E(\mu_{EC}(y_{EC}|_{AE}^+) - e_0 U_E^{\text{SCL}}) = \hat{L}_s^E(y_{EC}|_{AE}^+ \cdot e^{-\frac{e_0}{k_B T} U_E^{\text{SCL}}}) . \quad (55)$$

Another commonly used model is a functional dependency of L_s on the concentration $y_{AC}|_{AE}$ of intercalated ions at the interface, *i.e.* $L_s = L_s^A(y_{AC}|_{AE})$. Since the space charge layer in the active particle U_A^{SCL} is essentially constant (because μ_{Ae} is constant), we can indeed write

$$L_s = L_s^A(\mu_{AC}(y_{AC}|_{AE})) = \hat{L}_s^A(y_{AC}|_{AE}) . \quad (56)$$

We discuss this aspect as well as various models for $L_s(\mu_{AC}, \mu_{EC}, \mu_{ES}, \mu_{Ae})$ in section 4.2. Meanwhile we assume $L_s = \text{const.}$ and proceed the following derivation and the discussion based on this assumption since it turns out to be very reasonable.

2.8 Discussion of the model parameters

At this stage, it is illustrative to discuss the explicit value of the parameters.

- For the electrode geometry we consider for $\Sigma_{A,E}$ a planar surface of area A and a thickness $d_A = 10 [\mu\text{m}]$ which yields $V_A = A \cdot d_A$ and $x_{AE} = 10 [\mu\text{m}]$. The electrolyte is considered with a thickness of $d_E = 50 [\mu\text{m}]$. This corresponds to the cell dimensions of the cell MX-6 in [2].
- Throughout this work we consider DMC as solvent with $n_{ES}^R = 11.91 \left[\frac{\text{mol}}{\text{L}} \right]$ and assume for the solvation number $\kappa_E = 4$. The reference electrolyte concentration is $n_E^R = 1 \left[\frac{\text{mol}}{\text{L}} \right]$ and average amount of electrolyte is \bar{n}_E and a parameter of the model.
- Average concentrations (or mole fractions) are abbreviated as

$$\bar{y}_\alpha = \frac{1}{V_E} \int_{\Omega_E} y_\alpha dV \quad \alpha = E_C, E_A, E_S \quad (57)$$

for the electrolyte species and

$$\bar{y}_{AC} = \frac{1}{V_A} \int_{\Omega_A} y_{AC} dV \quad (58)$$

for the amount of intercalated ions in the active phase.

- For the active particle phase we consider $\text{Li}(\text{Ni}_{1/3}\text{Mn}_{1/3}\text{Co}_{1/3})\text{O}_2$ (NMC) whereby

$$q_A^{V,\text{NMC}} = 1294 \left[\frac{\text{mAh}}{\text{cm}^3} \right] \quad \text{and} \quad q_A^{V,\text{NMC}} = 318 \left[\text{mAh g}^{-1} \right] \quad (59)$$

which is simply computed from the density and stoichiometry of the bulk material[38]. As parameters for the chemical potential μ_{AC} we consider an occupation number of $\omega_A = 10$ and a Redlich–Kister interaction energy of $\gamma = 13$ [24].

- The differential capacity C_E^{DL} has a prescribed value (actually C_E^{DL} is a function of U_E^{SCL} , but we proceed here with a constant approximation for the sake of simplicity[9] of about

$$C_E^{\text{DL}} = 100 \left[\frac{\mu\text{F}}{\text{cm}^2} \right] \quad (60)$$

- The electrode capacity Q is

$$Q = \int_{\Omega_A} q_A^V \cdot y_{AC} dV = Q_A^V \cdot \bar{y}_{AC} \quad \text{with} \quad Q_A^V := V_A \cdot q_A^V \quad (61)$$

This yields the non-dimensional **capacity**

$$\frac{Q}{Q_A^V} = \bar{y}_{AC} \in (0, 1) \quad (62)$$

which is sometimes also called *status of charge* (SOC) or *depth of discharge* (DOD).

Note that during *discharge* of a complete battery the cathode is actually filled up with lithium. In a half cell with metallic lithium as counter electrode, *discharge* thus actually means *filling up* the intercalation electrode, here the NMC cathode material. Hence $Q/Q_A^V \rightarrow 0$ corresponds to a fully charged cathode (*i.e.* no lithium in the intercalation compound, $\bar{y}_{AC} \rightarrow 0$) while $Q/Q_A^V \rightarrow 1$ corresponds to a fully discharged cathode (*i.e.* the intercalation compound is completely filled with lithium, $\bar{y}_{AC} \rightarrow 1$).

- From the charge balance (35) of the active particle we can deduce

$$Q = Q^0 + \int_0^t I(t') dt \quad \text{with} \quad Q^0 = \int_{\Omega_A} q_A^V \cdot y_{AC}(\mathbf{x}, t=0) dV \quad (63)$$

where I is the current flowing into the intercalation electrode during *discharge* and $Q(t=0)$ the initial charge state. For a galvanostatic discharge $I > 0$ we obtain thus

$$Q = Q^0 + I \cdot t. \quad (64)$$

- The C-Rate C_h [1] defines (implicitly) the current at which after h -hours the intercalation cathode is completely filled during galvanostatic discharge. C_1 is thus the rate at which the battery is charged within one hour and commonly abbreviated just as C-rate C , *i.e.*

$$I_C = \frac{Q_A^V}{1 [\text{h}]} = A \frac{d_A \cdot q_A^V}{1 [\text{h}]}. \quad (65)$$

We can hence express the current I in multiples of the C-rate, *i.e.*

$$I = C_h \cdot I_C \quad (66)$$

which yields

$$Q = Q^0 + I \cdot t = Q^0 + C_h \cdot I_C \cdot t = Q^0 + C_h \cdot \frac{Q_A^V}{1 [\text{h}]} \cdot t = Q_A^V (y_{AC}^0 + C_h \frac{t}{[\text{h}]}) \quad (67)$$

The only parameter for the current density $i = I/A$ is thus C_h .

- For the time t we consider the interval of one discharge cycle, i.e. $t \in [0, t_{\text{end}}]$ with

$$t_{\text{end}} = \frac{1 [\text{h}]}{C_h} \quad (68)$$

We can thus introduce the non-dimensional time

$$\tau = C_h \frac{t}{3600 [\text{s}]} \in [0, 1] \quad (69)$$

whereby the capacity rewrites as

$$Q/Q_A^V = (y_{A_C}^0 + \tau) . \quad (70)$$

- For the current density i at the planar electrode we have thus

$$i = \frac{I}{A} = \frac{C_h \cdot I_C}{A} = i_A^C \cdot C_h \quad \text{with} \quad i_A^C := \frac{d_A \cdot q_A^V}{1 [\text{h}]} . \quad (71)$$

Discussion of the scaling Consider the non-dimensional voltage

$$\tilde{U} = \frac{e_0}{k_B T} U_E^{\text{SCL}} \quad (72)$$

and abbreviate

$$\tilde{H} = \frac{e_0}{k_B T} E_{A,R,E} - f_A + f_E \quad (73)$$

which yields

$$\tilde{U} - c_1 \cdot \frac{C_h}{\tilde{L}} \cdot \frac{d\tilde{U}}{d\tau} = \tilde{H}(1 - \tau) - \frac{C_h}{\tilde{L}} \quad (74)$$

with

$$c_1 := \frac{1}{d \cdot q_A^V} C_E^{\text{DL}} \frac{k_B T}{e_0} \quad (75)$$

The parameters $d_A = 0.01 [\text{cm}]$ and $q_A^V = 1294 [\text{mA h cm}^{-3}]$ yield

$$d \cdot q_A^V = 0.01 [\text{cm}] \cdot 1294 [\text{mA h cm}^{-3}] \cdot \frac{1}{[\text{h}]} = 12.94 \left[\frac{\text{mA h}}{\text{cm}^2} \right] \quad (76)$$

and

$$C_E^{\text{DL}} \frac{k_B T}{e_0} = 100 \left[\frac{\mu\text{F}}{\text{cm}^2} \right] \cdot 0.0257 [\text{V}] = 2.568 \left[\frac{\mu\text{C}}{\text{cm}^2} \right] \quad (77)$$

whereby

$$c_1 = 5.51 \cdot 10^{-8} . \quad (78)$$

The double layer contribution in eq. (51) is thus almost negligible whereby (51) reduces to

$$i = -e_0 L_s g\left(\frac{1}{k_B T_s} \lambda\right). \quad (79)$$

We consider for the exchange current density the rescaling

$$e_0 L_s = \tilde{L} \cdot i_A^C = \tilde{L} \frac{d_A \cdot q_A^V}{1 [\text{h}]}. \quad (80)$$

This is the crucial decomposition throughout this work and \tilde{L} the parameter of the surface reaction rate R_s .

For the current density $i = i_A^C \cdot C_h$ and the inverse function g^{-1} we obtain thus with eq. (48) for the surface affinity λ the general expression

$$E = E_{A,C} - \frac{k_B T}{e_0} (f_A - f_E|_{AE} + f_E|_{EC}) + \frac{k_B T}{e_0} g^{-1}\left(-\frac{C_h}{\tilde{L}}\right) - U_A^{\text{bulk}} + U_E^{\text{bulk}} \quad (81)$$

for the cell voltage E .

3 Discussion

If not stated otherwise, we abbreviate

$$y_{AC} = y_A \quad \text{and} \quad y_{EC} = y_E \quad (82)$$

as well as the respective densities $n_{AC} = n_A, n_{EC} = n_E$, fluxes $\mathbf{J}_{AC} = \mathbf{J}_A, \mathbf{J}_{EC} = \mathbf{J}_E$, and chemical potential $\mu_{AC} = \mu_A$ in the following.

We seek to discuss the general relation (81) of the cell voltage E as function of the capacity

$$\frac{Q}{Q_A^V} = \bar{y}_A \in (0, 1) \quad (83)$$

during discharge of an intercalation electrode. Note that necessarily $C_h > 0$ (discharge) and $\tilde{L} > 0$ (Onsager constraint of (38)), whereby $g^{-1}\left(-\frac{1}{2} \frac{C_h}{\tilde{L}}\right) < 0$, which entails that any current decreases the cell voltage E during discharge.

We will discuss consecutively the following hierarchy of approximations:

- BV 0:** infinite slow discharge - the open circuit potential
- BV 1:** infinite fast diffusion and conductivity in the active particle and the electrolyte
- BV 2:** finite conductivity in the active particle, infinite diffusion in the active particle, infinite fast diffusion and conductivity the electrolyte
- BV 3:** finite conductivity and diffusion in the active particle, infinite fast diffusion and conductivity the electrolyte
- BV 4:** finite conductivity and diffusion in the active particle, finite conductivity in the electrolyte, infinite fast diffusion the electrolyte
- BV 5:** finite conductivity in the active particle and the electrolyte, finite solid state diffusion in the intercalation electrode as well as finite diffusion in the electrolyte

3.1 BV 0: Open circuit potential

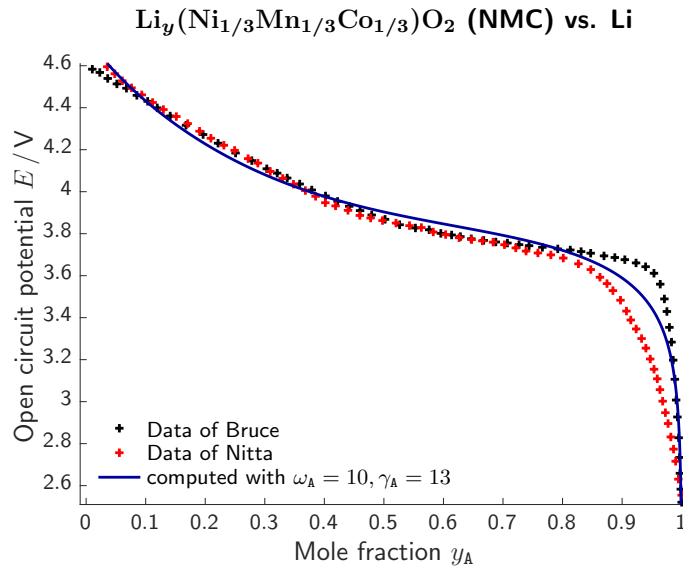


Figure 4: OCP of $\text{Li}_y(\text{Ni}_{1/3}\text{Mn}_{1/3}\text{Co}_{1/3})\text{O}_2$. Comparison between the material model (11) and experimental data of P. Bruce (Data of Fig. 3 in [39]) and N. Nitta *et. al* (Data of Fig. 4.e in [40]).

The open circuit potential (OCP) is obtained from (81) as

$$E = \frac{1}{e_0} (\mu_{C_C} - \mu_A(y_A)) \quad (84)$$

for $C_h = 0$ (infinite slow discharge), which entails also $U_A^{\text{bulk}} = U_E^{\text{bulk}} = 0$ as well as $y_E|_{\text{AE}} = y_E|_{\text{EC}}$. Hence we have

$$E = E_{A,C} - \frac{k_B T}{e_0} f_A(\bar{y}_A) = E^{(0)}(Q/Q_A^V). \quad (85)$$

For $\text{Li}_y(\text{Ni}_{1/3}\text{Mn}_{1/3}\text{Co}_{1/3})\text{O}_2$ [39] as intercalation electrode, the two parameters of the chemical potential function μ_A are the occupation number $\omega_A = 10$ and the interaction energy $\gamma_A = 13$ of the Redlich–Kister type enthalpy contribution. This yields an absolute ℓ^2 -error of 0.064 V and a relative error of 1.860% vs. experimental data of P. Bruce *et. al* [39], and Fig. 4 shows a comparison to two experimental data sets of measured OCP data.

3.2 BV 1: Infinite fast diffusion and conductivity in the active particle and the electrolyte

Infinite conductivity within the active particle phase as well as within the electrolyte yields

$$U_A^{\text{bulk}} = 0 \quad \text{and} \quad U_E^{\text{bulk}} = 0. \quad (86)$$

and infinite fast diffusion in the active particle and the electrolyte entails

$$y_A(x, t) = \text{const. w.r.t. } x \quad \text{and} \quad y_E(x, t) = \text{const. w.r.t. } x. \quad (87)$$

Hence $y_A|_{AE}$ is directly related to the capacity via

$$y_A|_{AE} = \bar{y}_A = Q/Q_A^V \quad (88)$$

whereby the cell voltage of **BV 1** is

$$E = E_{A,c} - \frac{k_B T}{e_0} f_A(\bar{y}_A) + \frac{k_B T}{e_0} g^{-1}\left(-\frac{C_h}{\tilde{L}}\right) =: E^{(1)}(Q/Q_A^V; C_h, \tilde{L}). \quad (89)$$

It is a simple algebraic relation between the measured cell voltage E , the C-rate C_h , the capacity Q and the (non-dimensional) exchange current density \tilde{L} .

In order to compare the cell voltage E computed in the approximation **BV 1** with other approximations, we abbreviate the voltage computed from (89) as $E^{(1)}$. Note that cell voltage (89) is actually *independent* of the electrolyte. $\tilde{L} = 1$ we obtain the voltage/capacity relation given in Fig. 5 for a variation of C_h from 0 (open circuit potential) to $C_h = 100$ (extremely fast discharge).

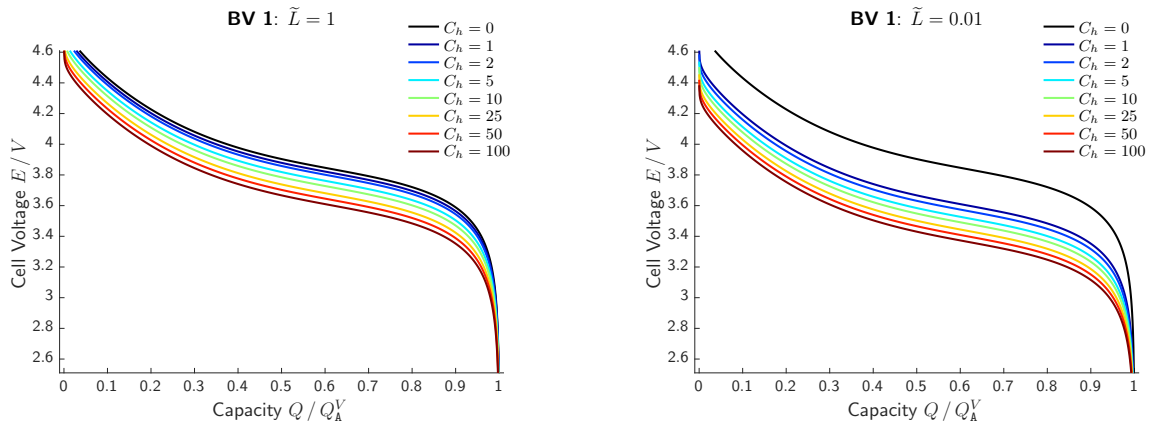


Figure 5: Computed voltage E as function of the capacity Q/Q_A according to eq. (89) for various values of \tilde{L} and C_h .

Reaction overpotential We define the *reaction overpotential* as

$$\eta^R = E^{(0)} - E^{(1)} = -\frac{k_B T}{e_0} g^{-1}\left(-\frac{C_h}{\tilde{L}}\right) \quad (90)$$

which is actually independent of the status of charge or capacity. Measured voltage data $\check{E} = \check{E}(C_h)$ would thus allow to determine \tilde{L} and the parameter $\alpha \in (0, 1)$.

Fig. 6 shows computations of the reaction overpotential η^R for various values of α and \tilde{L} as function of C_h .

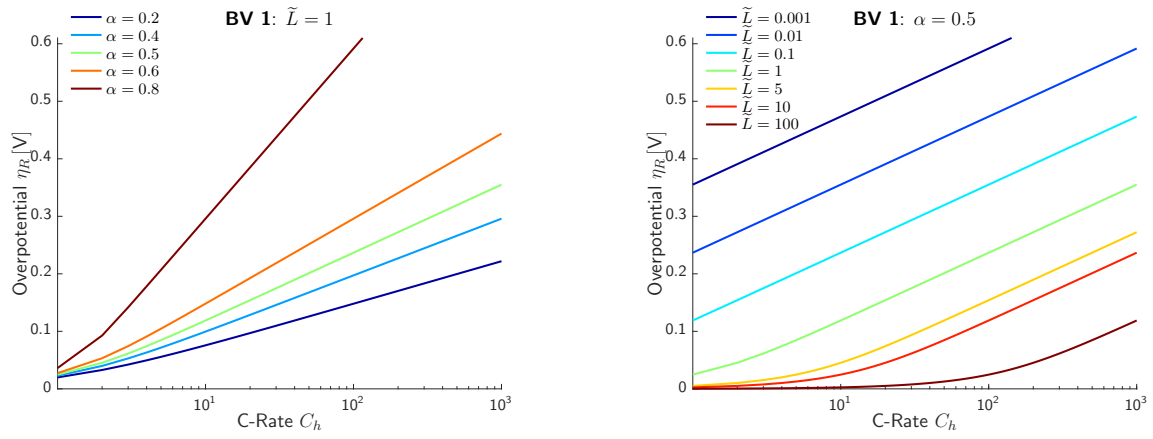


Figure 6: Reaction overpotential η^R as function of the C-Rate C_h with parameter variations of α and \tilde{L} .

3.3 BV 2: Contribution of finite active phase conductivity

Finite conductivity within active particle phase entails from eq. (35)

$$U_A^{\text{bulk}} = R_A^{\text{bulk}} \cdot i \quad \text{with} \quad R_A^{\text{bulk}} = \frac{d_A}{\sigma_A}. \quad (91)$$

Employing the scaling (71) of the current density i , i.e. $i = i_A^C \cdot C_h$, as well as the decomposition

$$\sigma_A = \sigma_A^C \cdot \tilde{\sigma}_A \quad \text{with} \quad \sigma_A^C := d_A \cdot i_A^C \cdot \frac{e_0}{k_B T} = \frac{d_A^2 q_A^V}{1 [h]} \cdot \frac{e_0}{k_B T} \quad (92)$$

yields

$$U_A^{\text{bulk}} = \frac{k_B T}{e_0} \frac{C_h}{\tilde{\sigma}_A}. \quad (93)$$

The quantity σ_A^C is the specific conductivity of the active particle phase at C-rate of one. For the parameters given in section 2.8 σ_A^C computes as

$$\sigma_A^C \approx 4.9 \left[\frac{\text{mS}}{\text{cm}} \right]. \quad (94)$$

The measured cell voltage is then

$$E = E_{A,C} - \frac{k_B T}{e_0} \left(f_A(\bar{y}_A) - g^{-1} \left(-\frac{C_h}{\tilde{L}} \right) + \frac{C_h}{\tilde{\sigma}_A} \right) =: E^{(2)}(Q/Q_A^V; C_h, \tilde{L}, \tilde{\sigma}_A) \quad (95)$$

which is (yet again) a simple algebraic relation between E , the C-rate C_h , and the capacity Q/Q_A^V . $E^{(2)}$ is additionally parametrically dependent on the conductivity $\tilde{\sigma}_A$.

We define the active phase conductivity overpotential η_A^σ as

$$\eta_A^\sigma := E^{(1)} - E^{(2)} = \frac{k_B T}{e_0} \frac{C_h}{\tilde{\sigma}_A}. \quad (96)$$

3.4 BV 3: Contribution of the solid-state diffusion in the active particle phase

Reconsider that we have assumed yet $y_A = \text{const.}$ with respect to space in the intercalation particle. In general, however, we have to solve a (here 1D) diffusion equation

$$\frac{\partial n_A}{\partial t} = -\partial_x j_A \quad \text{with} \quad j_A = -D_A n_A \partial_x f_A(y_A) \quad (97)$$

with

$$j_A|_{x=0}^+ = 0 \quad \text{and} \quad j_A|_{\text{AE}}^- = -\frac{1}{e_0} i. \quad (98)$$

This yields at the interface $\Sigma_{\text{A,E}}$ some solution

$$y_A(x, t)|_{x=x_{\text{AE}}} = y_A|_{\text{AE}}(t; i) \quad (99)$$

which will also impact the cell voltage

$$E = E_{\text{A,C}} - \frac{k_{\text{B}}T}{e_0} \left(f_A(y_A|_{\text{AE}}(t; i)) - g^{-1}\left(-\frac{C_h}{\tilde{L}}\right) + \frac{C_h}{\tilde{\sigma}_A} \right) \quad (100)$$

$$E^{(3)}(Q/Q_{\text{A}}^V; C_h, \tilde{L}, \tilde{\sigma}_A, \tilde{D}_A). \quad (101)$$

In order to discuss this impact systematically, we apply the following scaling

$$\tau = C_h \frac{t}{[h]} \in [0, 1] \quad \text{and} \quad \xi = \frac{x}{d_A} \in [0, 1] \quad (102)$$

as well as

$$n_A = y_A \cdot \frac{q_{\text{A}}^V}{e_0} \quad \text{and} \quad \tilde{j}_A = \frac{1}{L_s} j_A \quad (103)$$

which leads to

$$\frac{C_h}{\tilde{L}} \frac{\partial y_A}{\partial t} = -\partial_{\xi} \tilde{j}_A. \quad (104)$$

The dimensionless flux

$$\tilde{j}_A = \frac{1}{\tilde{L}} j_A = -\frac{1}{\tilde{L}} \frac{1 [h]}{d^2} D_A y_A \partial_{\xi} f_A(y_A) \quad (105)$$

yields the dimensionless diffusion coefficient

$$\tilde{D}_A = \frac{1 [h]}{d^2} D_A \quad (106)$$

and thus

$$\tilde{j}_A = -\frac{\tilde{D}_A}{\tilde{L}} y_A \partial_{\xi} f_A(y_A) \quad (107)$$

At the interface $\Sigma_{A,E}$ we have thus

$$\tilde{j}_A \Big|_{\xi=1} = -\frac{C_h}{\tilde{L}}. \quad (108)$$

Overall we may write

$$\frac{C_h}{\tilde{D}_A} \frac{\partial y_A}{\partial \tau} = \partial_\xi \left(y_A \frac{\partial f_A}{\partial y_A} \partial_\xi y_A \right) \quad (109)$$

with

$$y_A \frac{\partial f_A}{\partial y_A} \partial_\xi y_A \Big|_{\xi=0} = 0 \quad \text{and} \quad y_A \frac{\partial f_A}{\partial y_A} \partial_\xi y_A \Big|_{\xi=1} = \frac{C_h}{\tilde{D}_A}. \quad (110)$$

Note that we can analytically compute $y_A \frac{\partial f_A}{\partial y_A} = \Gamma_A^{\text{tf}}(y_A)$ from eq. (11) (see also appendix B.1) as

$$\Gamma_A^{\text{tf}} = y_A \cdot \frac{\partial f_A}{\partial y_A} = \frac{1}{(1-y_A)(\frac{1}{\omega_A} y_A + (1-y_A))} + \gamma_A \cdot (16 \cdot y_A^3 - 22 y_A^2 + \frac{25}{3} y_A). \quad (111)$$

Since the problem (109) is non-linear, a classical separation *Ansatz* $y_A = X(\xi) \cdot T(\tau)$ is not meaningful. We proceed thus with solving the problem (109) with (110) numerically with MATLAB[®] and the `pdepde()` function. The syntax for `pdepde()` of the problem (109) with (110) is given in appendix B.2.

Based on the numerical solution $\hat{y}_A(\xi, \tau)$ we compute then $y_A \Big|_{AE} = \hat{y}_A(\xi, \tau) \Big|_{\xi=1}(\tau; C_h, \tilde{D}_A)$ numerically for various values of C_h and \tilde{D}_A . The (global) capacity is yet $Q/Q_A^V = \bar{y}_A = \tau$.

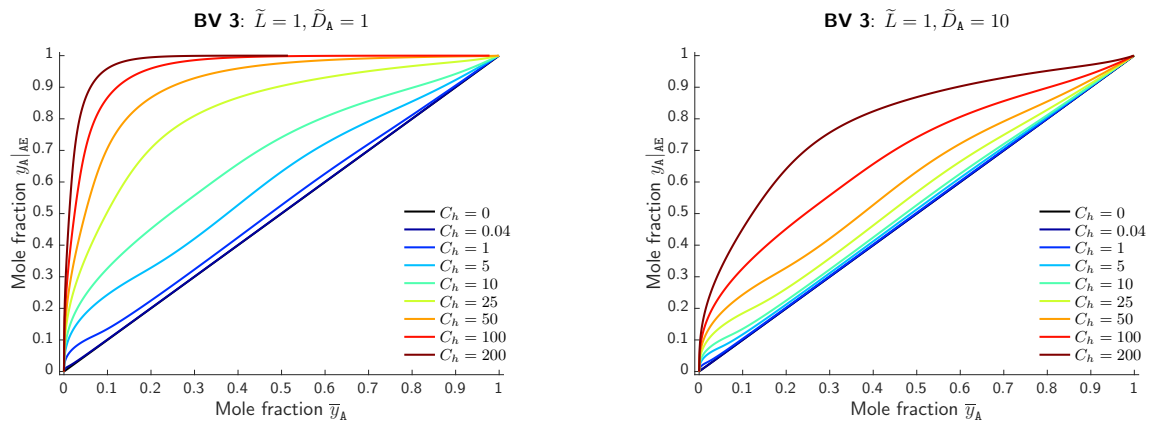


Figure 7: Concentration $y_A \Big|_{AE} = \hat{y}_A \Big|_{AE}$ of intercalated ions at the interface $\Sigma_{A,E}$ as function the status of discharge Q/Q_A^V for various values of C_h and \tilde{D}_A .

We assume the same parameters as before, now additionally with two values of the diffusion coefficient \tilde{D}_A , *i.e.* slow diffusion $\tilde{D}_A = 1$ and fast diffusion $\tilde{D}_A = 10$, and compute $y_A \Big|_{AE}$ as function of the capacity Q/Q_A^V (or time τ). Fig. 7 shows computations of $y_A \Big|_{AE}$ for various discharge rates and diffusion coefficients in the active particle phase as function of the cell capacity. The angle bisection in black corresponds to the open circuit potential situation, where $y_A \Big|_{AE} = \bar{y}_A$. For increasing discharge rates, the concentration $y_A \Big|_{AE}$ at the interface $\Sigma_{A,E}$ is larger

than the average concentration \bar{y}_A in Ω_A since the evacuation of intercalated ions is delayed by the finite diffusion. This effect becomes even stronger for smaller values of \widetilde{D}_A , i.e. slow diffusion in the active particle.

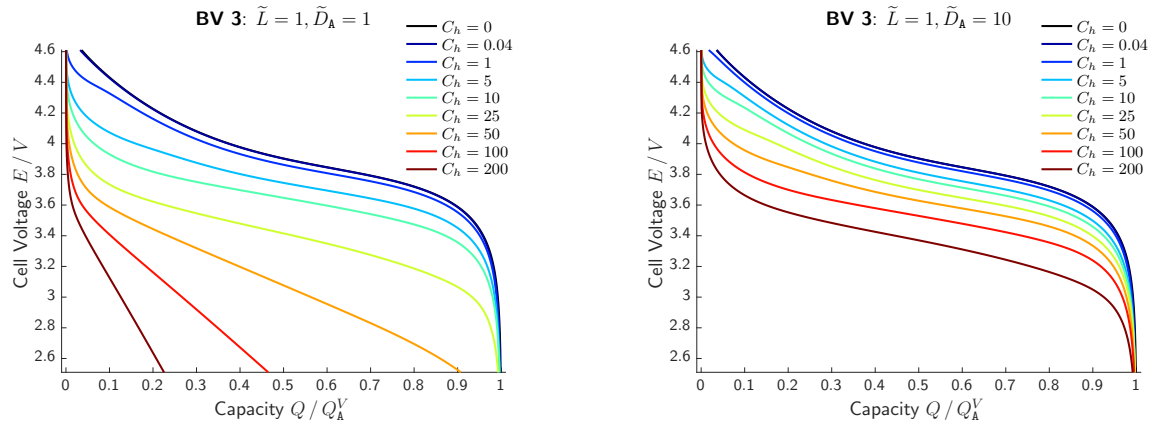


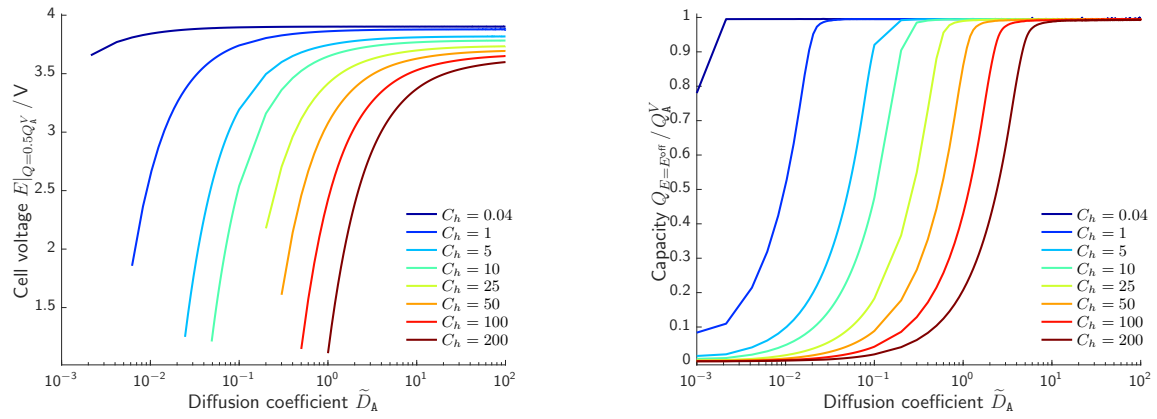
Figure 8: Cell voltage E for **BV 3** as function of the status of discharge for various values of C_h and \widetilde{D}_A with numerical computation of $\hat{y}_{A,0}(i)$ from the PDE (109) with boundary conditions (110).

The cell voltage E is then computed *a posteriori* from (100) based on the numerical solution of $y_A|_{AE}$. Fig. 8 displays the cell voltage for various discharge rates as well as slow ($\widetilde{D}_A = 1$) and fast ($\widetilde{D}_A = 10$) diffusion in the intercalation phase. Finite diffusion in the active particle has an enormous impact on the cell voltage and changes qualitatively the shape due to the non-linear feedback. This effect is also found experimentally, see Fig. 1, and extremely important since it determines the maximum amount of charge that can be withdrawn from an intercalation electrode.

Two important measures server to discuss the impact of the diffusion coefficient \widetilde{D}_A ,

- the cell voltage at 50% discharge, i.e. $E|_{Q=0.5 \cdot Q_A^V}$,
- and the capacity $Q|_{E=E^{\text{off}}}$ at the cut off voltage E^{off} , here with $E^{\text{off}} = 2.6 / V$.

Fig 9 shows numerical computations of $E|_{Q=0.5 \cdot Q_A^V}$ and $Q|_{E=E^{\text{off}}}$ for various values of the C-rate C_h and diffusion coefficients \widetilde{D}_A in the range of $10^{-3} - 10^2$. For slow discharge rates, i.e. $C_h < 1$ a diffusion coefficient of $\widetilde{D}_A = 0.1$ is sufficient to achieve a voltage of 3 / V at 50% discharge and capacity of 90% at the the cutoff voltage. However, for higher C-rates, e.g. $C_h = 50$, the impact of the solid state diffusion becomes enormous, **requiring** a diffusion coefficient of $\widetilde{D}_A > 0.3$ to discharge the electrode to 50%.



(a) Cell voltage at 50% state of discharge.

(b) Capacity at the cutoff voltage $E^{\text{off}} = 2.6 / \text{V}$

Figure 9: Cell voltage and Capacity for various discharge rates and diffusion coefficients.

Overpotential η_A^D : The *overpotential* due to finite diffusion in the active particle phase can be defined as

$$\eta_A^D := E^{(2)} - E^{(3)} \quad (112)$$

which computes as

$$\eta_A^D = -\frac{k_B T}{e_0} \left(f_A(\bar{y}_A) - f_A(\hat{y}_A|_{AE}) \right). \quad (113)$$

Fig. 10 shows computations of η_A^D for slow and fast diffusion. The

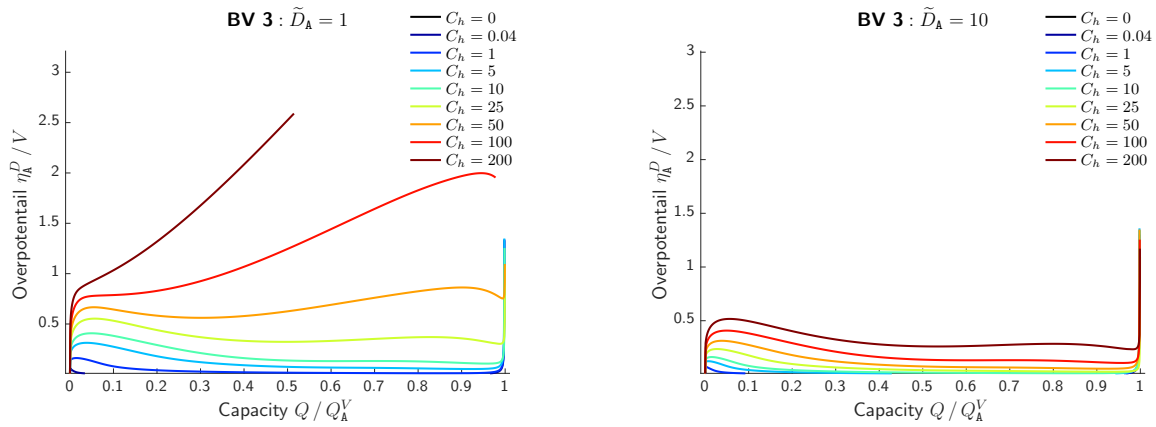


Figure 10: Overpotential η_A^D as function of the status of discharge Q/Q_A^V for slow ($\tilde{D}_A = 1$) and fast ($\tilde{D}_A = 10$) diffusion in the intercalation phase.

3.5 BV 4: Finite conductivity in the electrolyte

First note that an infinite fast diffusion in the electrolyte yet entails $y_E = \bar{y}_E$, whereby the (coupled) transport equation system (23) – (24) of the electrolyte reduces to

$$i = -\Lambda_E n_E \partial_x \varphi_E, \quad (114)$$

which yields

$$U_E^{\text{bulk}} = -R_E^{\text{bulk}} \cdot i \quad \text{with} \quad R_E^{\text{bulk}} = \frac{d_E}{\Lambda_E n_E}. \quad (115)$$

Employing the scaling (71) of the current density i , *i.e.* $i = i_A^C C_h$ yields

$$U_E^{\text{bulk}} = -\frac{d_E}{\Lambda_E n_E} \cdot i_A^C C_h = \frac{d_E}{d_A} \frac{\sigma_A^C}{\Lambda_E n_E} \frac{k_B T}{e_0} C_h, \quad (116)$$

which motivates the decomposition

$$\Lambda_E n_E^R = \sigma_E^R = \sigma_A^C \cdot \tilde{\sigma}_E \quad \text{with} \quad \sigma_A^C = d_A \cdot i_A^C \cdot \frac{e_0}{k_B T} = \frac{d_A^2 q_A^V}{1 [h]} \cdot \frac{e_0}{k_B T}. \quad (117)$$

Here n_E^R is a constant reference electrolyte concentration, *e.g.* 1 mol L^{-1} , and $\sigma_E^R = \Lambda_E n_E^R$ is the corresponding reference conductivity. Hence

$$U_E^{\text{bulk}} = -\tilde{d} \cdot \tilde{c}_E^R \cdot \frac{k_B T}{e_0} \frac{C_h}{\tilde{\sigma}_E} \quad \text{with} \quad \tilde{d} := \frac{d_E}{d_A} \quad \text{and} \quad \tilde{c}_E^R := \left(\frac{n_E^R}{n_E} \right), \quad (118)$$

whereby the cell voltage is

$$E = E_{A,C} - \frac{k_B T}{e_0} \left(f_A(y_A|_{AE}(t; i)) - g^{-1} \left(-\frac{C_h}{\tilde{L}} \right) + \frac{C_h}{\tilde{\sigma}_A} + \tilde{d} \tilde{c}_E^R \frac{C_h}{\tilde{\sigma}_E} \right) \quad (119)$$

$$= E^{(4)}(Q/Q_A^V; C_h, \tilde{L}, \tilde{\sigma}_A, \tilde{D}_A, \tilde{\sigma}_E, \tilde{d}, \tilde{c}_E^R). \quad (120)$$

Hence, finite conductivity in the electrolyte linearly decreases the cell voltage and scales also with the ratio of the electrode width to the electrolyte width, *i.e.* \tilde{d} . The quantity \tilde{c}_E^R accounts for concentration dependence of the electrolyte conductivity.

Correspondingly we define the electrolyte conductivity overpotential η_E^Λ as

$$\eta_E^\sigma := E^{(3)} - E^{(4)} = \frac{k_B T}{e_0} \tilde{d} \tilde{c}_E^R \frac{C_h}{\tilde{\sigma}_E}. \quad (121)$$

3.6 BV 5: Finite diffusion in the electrolyte phase

The final contribution to the surface reaction R is the space dependent electrolyte concentration. We have yet assumed $y_E = \text{const.}$ with respect to space, however, in general the (coupled) equation system (23) – (24) has to be solved.

Note that $t_{EC} = \text{const.}$ simplifies the (coupled) equation system (23) – (24) to

$$\frac{\partial n_E}{\partial t} = \partial_x \left(D_E \cdot n_E^{\text{tot}} \Gamma_E^{\text{tf}} \cdot \partial_x y_E \right) \quad (122)$$

$$i = -S_E \cdot n_E^{\text{tot}} \Gamma_E^{\text{tf}} \partial_x y_E - \Lambda_E n_E \partial_x \varphi_E. \quad (123)$$

Further, $J_E = -D_E \cdot n_E^{\text{tot}} \Gamma_E^{\text{tf}} \cdot \partial_x y_E + \frac{t_{EC}}{e_0} i$ entails at the interface $\Sigma_{A,E}$ the condition

$$-D_E \cdot n_E^{\text{tot}} \Gamma_E^{\text{tf}} \cdot \partial_x y_E \Big|_{AE} = \frac{1 - t_{EC}}{e_0} i \quad (124)$$

We assume that the average electrolyte concentration n_E is constant in time, *i.e.*

$$\frac{\partial \bar{n}_E}{\partial t} = 0 \quad \text{with} \quad \bar{n}_E = \frac{1}{d_E} \int_{x_{EC}}^{x_{AE}} n_E, dx . \quad (125)$$

which yields at the right boundary $x = x_{EC}$ the condition

$$D_E \cdot n_E^{\text{tot}} \Gamma_E^{\text{tf}} \cdot \partial_x y_E \Big|_{x=x_{EC}} = \frac{1 - t_{EC}}{e_0} i . \quad (126)$$

The concept of an *ideally polarizable* counter-electrode Ω_C , positioned at $x = x_{EC}$, delivers (or consumes) hence exactly the amount of ions in the electrolyte which flow in (or out) of Ω_E at $x = x_{AE}$, with keeping the reaction 45 in thermodynamic equilibrium. The initial value is

$$y_E(x, t = 0) = y_E(\bar{n}_E) \quad (127)$$

where \bar{n}_E is the prescribed *average* electrolyte concentration.

We introduce the scalings

$$\tau = C_h \frac{t}{[h]} \in [0, 1] , \quad \xi = \frac{x}{d_E} \in [0, 1] , \quad \frac{n_E^{\text{tot}}(\xi, \tau)}{n_E^R} =: \tilde{c}_E^{\text{tot},R}(\xi, \tau) \quad (128)$$

$$\Lambda_E n_E^R = \tilde{\sigma}_E \cdot \sigma_A^C , \quad i = i_C \cdot C_h , \quad \tilde{d} = \frac{d_E}{d_A} \quad (129)$$

with $\sigma_A^C = d_A \cdot i_A^C \cdot \frac{e_0}{k_B T}$ and $i_A^C = \frac{d_A \cdot q_A^V}{1 [h]}$. This yields for (122)

$$C_h \frac{d_E^2}{1 [h]} \cdot \frac{1}{D_E} \cdot h_E \cdot \frac{\partial y_E}{\partial \tau} = \partial_\xi (\tilde{c}_E^{\text{tot},R} \Gamma_E^{\text{tf}} \cdot \partial_\xi y_E) \quad \text{with} \quad h_E := \frac{1}{n_E^R} \frac{\partial n_E}{\partial y_E} . \quad (130)$$

The corresponding non-dimensional boundary conditions at $\xi = 0$ reads

$$(\tilde{c}_E^{\text{tot},R} \Gamma_E^{\text{tf}} \partial_\xi y_E) \Big|_{\xi=0} = d_E \frac{1}{n_E^R} \frac{1}{D_E} \frac{1 - t_{EC}}{e_0} \cdot i \quad (131)$$

which introduces (implicitly) the scaling

$$D_E = \tilde{D}_E \cdot \left(\frac{q_A^V}{e_0 n_E^R} (1 - t_{EC}) \cdot \frac{d_A d_E}{1 [h]} \right) \quad (132)$$

leaving

$$(\tilde{c}_E^{\text{tot},R} \Gamma_E^{\text{tf}} \partial_\xi y_E) \Big|_{\xi=0} = \frac{C_h}{\tilde{D}_E} \quad \text{and} \quad (\tilde{c}_E^{\text{tot},R} \Gamma_E^{\text{tf}} \partial_\xi y_E) \Big|_{\xi=1} = \frac{C_h}{\tilde{D}_E} . \quad (133)$$

The balance equation (122) then reads

$$\tilde{d} \cdot \tilde{q}^V \cdot \tilde{t}_E \frac{C_h}{\tilde{D}_E} h_E(y_E) \frac{\partial y_E}{\partial \tau} = \partial_\xi (\tilde{c}_E^{\text{tot},R} \Gamma_E^{\text{tf}} \cdot \partial_\xi y_E) \quad (134)$$

with

$$\tilde{q}^V := \frac{q_E^V}{q_A^V} , \quad q_E^V = 2e_0 n_E^R \quad \text{and} \quad \tilde{t}_E = \frac{1}{2 \cdot (1 - t_{EC})} . \quad (135)$$

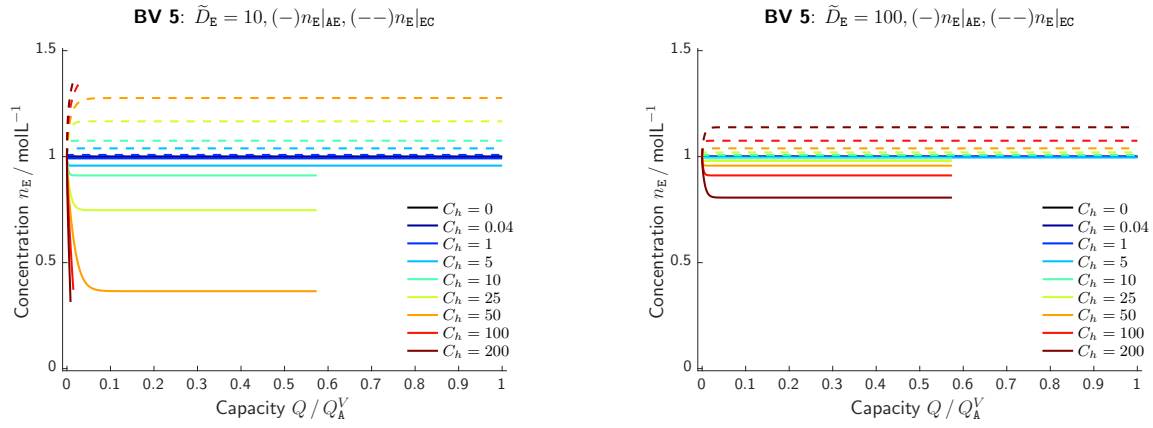


Figure 11: Numerical computation of the cation interface concentrations $n_E|_{AE}$ and $n_E|_{EC}$ in the electrolyte for slow ($\tilde{D}_E = 10$) and fast ($\tilde{D}_E = 100$) diffusion and various C-rates C_h .

Note that the 2 in q_E^V accounts for the charge of cations and anions. The charge capacity q_E^V of a 1 mol L^{-1} electrolyte is

$$q_E^V = 2e_0 n_E^R \approx 53 \text{ [mA h cm}^{-3}] \quad (136)$$

whereby

$$\tilde{q}^V = \frac{45}{1294} = 0.042553. \quad (137)$$

The dimensionless transference number $\tilde{t}_E \approx 1$ and $\tilde{d} = 5$. The PDE is solved with MATLAB's `pdepe` function, and details are given in the appendix A.3. We denote the numerical solution of y_E with \hat{y}_E and emphasize that the capacity is yet $Q/Q_A^V = \tau$. The numerical solutions \hat{y}_E at the respective boundaries $x = x_{AE}$ and $x = x_{EC}$ are

$$y_E|_{AE}^+ = \hat{y}_E|_{\xi=0} \quad \text{and} \quad y_E|_{EC}^- = \hat{y}_E|_{\xi=1}. \quad (138)$$

We discuss now briefly the concentration distribution in the electrolyte as function of the C-rate C_h and the diffusion coefficient \tilde{D}_E based on numerical solutions of (122) with boundary conditions (124) and (126).

Fig. 11 displays computations of the electrolytic cation concentration at the interface $\Sigma_{A,E}$ of the intercalation electrode, *i.e.* $n_E|_{AE}$, and at the interface $\Sigma_{E,C}$ of the counter electrode, *i.e.* $n_E|_{EC}$ for slow electrolytic diffusion ($\tilde{D}_E = 1$, left) and fast diffusion ($\tilde{D}_E = 10$, right) for various values of the C-rate.

After a short time the concentration yields a stationary state and Fig. 12 displays the stationary concentration $n_E(x)$ in the electrolyte, again for slow and fast diffusion as well as for various C-rates.

Note, however, that the concentration variation of y_E has additionally an impact on the voltage drop U_E . First reconsider that (123) rewrites as

$$U_E = -\frac{d_E}{\Lambda_E n_E^R} \left(\frac{1}{d_E} \int_{x_{EC}}^{x_{AE}} \frac{n_E^R}{n_E} dx \right) \cdot i + \frac{k_B T}{e_0} (2t_C - 1) (f_E(y_E|_{AE}) - f_E(y_E|_{EC})). \quad (139)$$

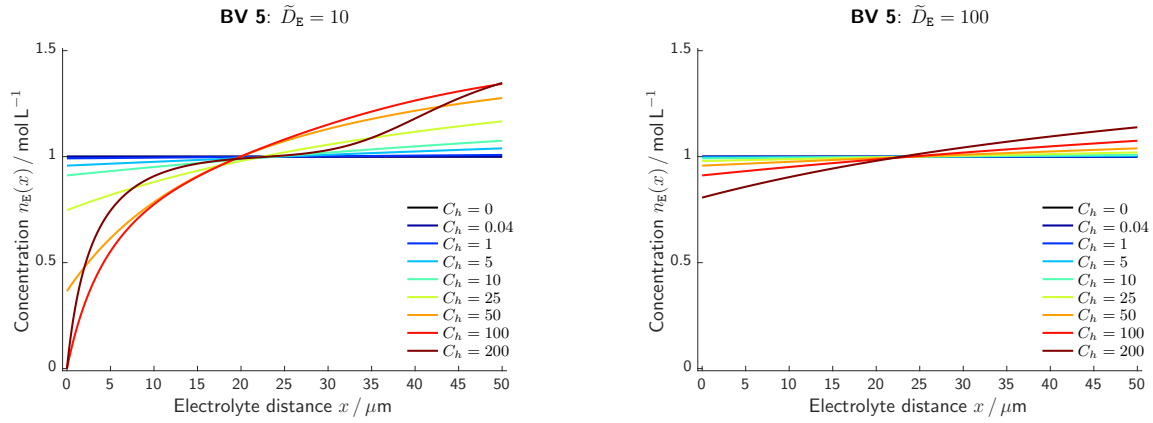


Figure 12: Numerical computation of the stationary cation distribution in the electrolyte for slow ($\tilde{D}_E = 10$) and fast ($\tilde{D}_E = 100$) diffusion and various C-rates C_h

since

$$\frac{S_E}{\Lambda_E} = \frac{k_B T}{e_0} (2t_C - 1). \quad (140)$$

We abbreviate

$$\tilde{c}_E^R := \left(\frac{1}{d_E} \int_{x_{EC}}^{x_{AE}} \frac{n_E^R}{n_E} dx \right) = \tilde{c}_E^R \quad (141)$$

and insert the scaling $\Lambda_E n_E^R = \tilde{\sigma}_E \cdot \sigma_A^C$ which yields

$$U_E = -\tilde{d} \tilde{c}_E^R \cdot \frac{k_B T}{e_0} \frac{C_h}{\tilde{\sigma}_E} + \frac{k_B T}{e_0} (2t_C - 1) (f_E(y_E|_{AE}) - f_E(y_E|_{EC})). \quad (142)$$

The overall cell voltage of **BV 5** is then

$$E = E_{A,C} - \frac{k_B T}{e_0} \left(f_A(\hat{y}_A|_{AE}) - 2 \cdot t_C (f_E(\hat{y}_E|_{AE}) - f_E(\hat{y}_E|_{EC})) - g^{-1} \left(-\frac{C_h}{\tilde{L}} \right) + \frac{C_h}{\tilde{\sigma}_A} + \tilde{d} \tilde{c}_E^R \frac{C_h}{\tilde{\sigma}_E} \right) \quad (143)$$

$$= E^{(5)}(s, C_h; \tilde{L}, \tilde{\sigma}_A, \tilde{D}_A, \tilde{\sigma}_E, \tilde{D}_E, t_{EC}, \tilde{d}, \tilde{n}_E). \quad (144)$$

In order to show the impact of the electrolyte concentration variation on the cell voltage E , assume for a moment $U_E^{\text{bulk}} = U_A^{\text{bulk}} = 0$ as well infinite fast diffusion in the active particle phase Ω_A . This yields

$$E = E_{A,C} - \frac{k_B T}{e_0} \left(f_A(\bar{y}_A) - 2 \cdot t_C (f_E(\hat{y}_E|_{AE}) - f_E(\hat{y}_E|_{EC})) - g^{-1} \left(-\frac{C_h}{\tilde{L}} \right) \right) \quad (145)$$

and numerical computations of the cell voltage for slow and fast diffusion are shown in Fig. 13.

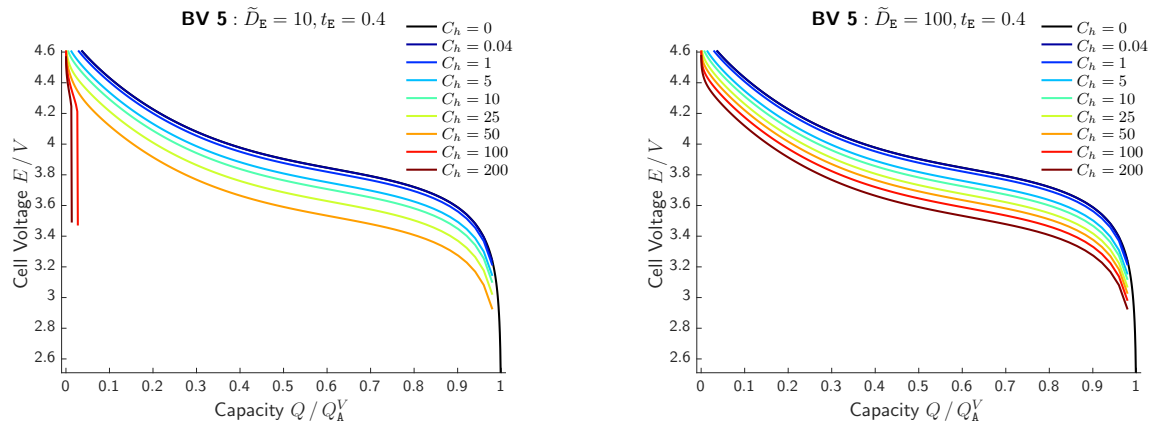


Figure 13: Computed cell voltage according to (145) with numerical solutions shown in Fig. 11 of the interface concentrations $\hat{y}_E|_{AE}$ and $\hat{y}_E|_{EC}$ for various discharge rates.

Overpotential Due to the (stationary) concentration gradients in the electrolyte (c.f. Fig. 12) we have a diffusional overpotential η_E^D , which can be defined as

$$\eta_E^\sigma := E^{(4)} - E^{(5)} = \frac{k_B T}{e_0} \left(\tilde{d} (\tilde{c}_E^R - \tilde{c}_E^L) \frac{C_h}{\tilde{\sigma}_E} - 2 \cdot t_C (f_E(\hat{y}_E|_{AE}) - f_E(\hat{y}_E|_{EC})) \right) \quad (146)$$

$$\approx -\frac{k_B T}{e_0} 2 \cdot t_C (f_E(\hat{y}_E|_{AE}) - f_E(\hat{y}_E|_{EC})) \quad (147)$$

Fig. 14 displays numerical computations of the overpotential η_E^D for slow and fast diffusion in the electrolyte.

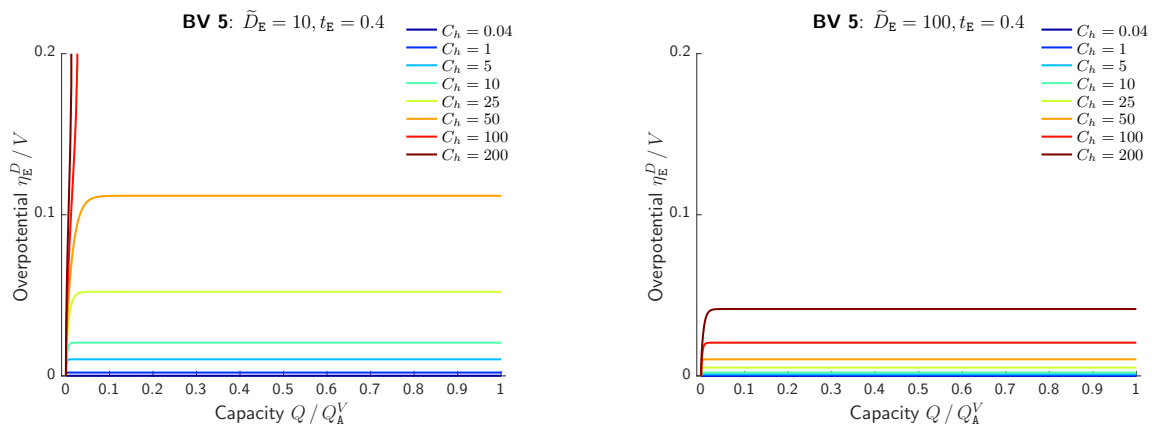


Figure 14: Diffusional overpotential of the electrolyte for slow and fast diffusion computed from numerical solutions of the interface concentrations $\hat{y}_E|_{AE}$ and $\hat{y}_E|_{EC}$ and eq. (146).

The *recursive* definition of the various overpotentials allows us to write

$$E = E^{(0)}(\bar{y}_A) - \eta^R - \eta_A^D - \eta_A^\sigma - \eta_E^D - \eta_E^\sigma \quad (148)$$

with one overpotential for each non-equilibrium process, measuring the deviation from the equilibrium of the respective process. This decomposition is hence a useful tool to systematically investigate the contribution of each process in broadly conceived experimental or numerical studies of a cell batch with varying parameters.

Internal resistance Note that we can also compute the internal resistance R^{int} of the electrochemical cell via the implicit definition

$$E - E^{(0)} = R \cdot I . \quad (149)$$

With $I = \frac{i_A^C \cdot C_h}{A}$ we obtain for the specific resistance

$$R = \frac{E - E^{(0)}}{I} = -\frac{A}{i_A^C} \frac{(\eta^R + \eta_A^D + \eta_A^\sigma + \eta_E^D + \eta_A^\sigma)}{C_h} = R_A \cdot (r^R + r_A^D + r_A^\Sigma + r_E^D + r_E^\sigma) \quad (150)$$

with

$$R_A = \frac{k_B T}{e_0} \frac{A}{i_A^C} \quad (151)$$

and

- intercalation reaction resistance

$$r^R = -g^{-1} \left(-\frac{C_h}{\tilde{L}} \right) \frac{1}{C_h} \stackrel{\text{Tafel}}{\approx} \frac{1}{\tilde{L}} , \quad (152)$$

- active phase diffusional resistance

$$r_A^D = \left(f_A(\bar{y}_A) - f_A(\hat{y}_A|_{\text{AE}}) \right) \frac{1}{C_h} , \quad (153)$$

- active phase conduction resistance

$$r_A^\sigma = \frac{1}{\tilde{\sigma}_A} , \quad (154)$$

- electrolyte diffusional resistance

$$r_E^D = 2 \cdot t_C \left(f_E(\hat{y}_E|_{\text{AE}}) - f_E(\hat{y}_E|_{\text{EC}}) \right) \cdot \frac{1}{C_h} , \quad (155)$$

- electrolyte conduction resistance

$$r_E^\sigma = \frac{1}{\tilde{\sigma}_E} . \quad (156)$$

4 Conclusion

4.1 Validation

Equation (143) for the general relation for the cell voltage E in a simple, non-porous intercalation electrode. Note, however, that the scalings, discussion and parameter study of section 3 can be straight forward adapted to porous electrodes.

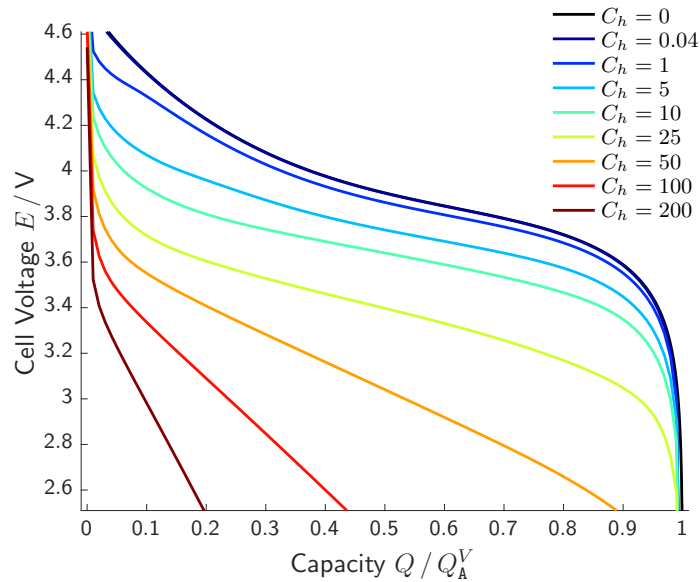


Figure 15: Computed cell voltage E as function of the capacity Q/Q_A^V with parameters of the non-equilibrium processes according to (157).

We provide finally a validation study for NMC with the following set of the non-dimensional parameters

$$\tilde{L} = 1, \quad \tilde{D}_A = 1, \quad \sigma_A = 100, \quad \tilde{D}_E = 100, \quad \tilde{\sigma}_E = 500. \quad (157)$$

Figure 15 displays the numerical computation of the cell voltage. In comparison to experimental data for a cell of the same dimension (however, neglecting porosity), we obtain a good qualitative and quantitative agreement to Fig 1.

This is especially remarkable since we assumed essentially for all non-equilibrium parameters constant values, *i.e.* no concentration dependence of the diffusion coefficients D_A and D_E , the cation transference number t_E , and the conductivities. In particular we assumed that the exchange current density $e_0 L_s$ is also constant, yielding the reasonable results of the last section. Note, however, that it is frequently assumed that the exchange current density is dependent on cation concentration at the interface $\Sigma_{A,E}$. We discuss this aspect in the next section and emphasize again that a consistent thermodynamic modeling as well as coupling through the surface reaction rate yields the reasonable results of the last sections. The scaling of all non-equilibrium parameters to the C-rate is quite illustrative for the sake of galvanostatic discharge and especially for the systematic *search* of the parameters of a specific battery.

4.2 Discussion of the exchange current density

The preceding discussion of the cell voltage E was based on the model (38) of the surface reaction rate R_s , *i.e.*

$$R_s = L_s \cdot \left(e^{\alpha \cdot \frac{1}{k_B T} \lambda} - e^{-(1-\alpha) \cdot \frac{1}{k_B T} \lambda} \right) \quad \text{with} \quad \lambda_s = \mu_{sA_C} + \kappa_E \cdot \mu_{sE_S} - \mu_{sE_C} - \mu_{sA_e}, \quad (158)$$

with $L_s = \text{const.}$ In section 81 we showed that double layer charging effects are negligible under galvanostatic conditions, whereby the measurable current density i is directly related to $e_0 R_s$,

i.e. $i = r_0 R_s$. The surface affinity λ is related to the cell voltage E via (48), i.e.

$$\lambda = e_0(E + U_A^{\text{bulk}} - U_E^{\text{bulk}} - E_{A,C}) + k_B T (f_A - f_E|_{AE} + f_E|_{EC}) \quad (159)$$

with

$$f_E(y_E) := \ln \left(\frac{y_E}{(\hat{y}_{E,S}(y_E))^{\kappa_E}} \right), \quad (160)$$

$$f_A(y_A) := \ln \left(\frac{\frac{1}{\omega_A} y_A}{1 + \frac{1-\omega_A}{\omega_A} y_A} \right) - \omega_A \cdot \ln \left(\frac{1 - y_A}{1 + \frac{1-\omega_A}{\omega_A} y_A} \right) + \gamma_A \cdot g_A(y_A). \quad (161)$$

Note that we have introduced the open circuit potential $E^{(0)}$ in section 3.1 as

$$E^{(0)}(\bar{y}_A) = E_{A,C} - \frac{k_B T}{e_0} f_A(\bar{y}_A). \quad (162)$$

We can also evaluate the open circuit potential function $E^{(0)}$ with the interface concentration $y_A|_{AE}$, i.e.

$$E^{(0)}(y_{AE}) = E_{A,C} - \frac{k_B T}{e_0} f_A(y_{AE}). \quad (163)$$

Note that this is a crucially different to (162) when finite diffusion in the active particle phase is considered, see section 3.2. However, this allows us rewrite the surface affinity λ as

$$\lambda = e_0(\varphi_A - \varphi_E - E^{(0)}(y_A|_{AE})) - k_B T f_E|_{AE} \quad (164)$$

$$= e_0(\varphi_A - \tilde{\varphi}_E - E^{(0)}(y_A|_{AE})) = e_0(\tilde{\eta}_{AE} - E^{(0)}(y_A|_{AE})) \quad (165)$$

with

$$\varphi_A = \varphi|_{AE}^-, \quad \varphi_E = \varphi|_{AE}^+, \quad \tilde{\varphi}_E := \varphi|_{AE}^+ + \frac{k_B T}{E_0} f_E(y_E|_{AE}) \quad (166)$$

and

$$\eta_{AE} := \varphi_A - \tilde{\varphi}_E = U_{AE}^{\text{DL}} - \frac{k_B T}{e_0} f_E|_{AE}. \quad (167)$$

This yields

$$i = e_0 L_s \cdot \left(e^{\alpha \cdot \frac{e_0}{k_B T} (\tilde{\eta}_{AE} - E^{(0)}(y_A|_{AE}))} - e^{-(1-\alpha) \cdot \frac{e_0}{k_B T} (\tilde{\eta}_{AE} - E^{(0)}(y_A|_{AE}))} \right). \quad (168)$$

This is the general, thermodynamic consistent version of the Butler–Volmer-equation [4, 26]. The specific form (168) of the current density i in terms of the *surface overpotential* [1] η_{AE} , the open circuit potential $E^{(0)}(y_A|_{AE})$, and the exchange current density $e_0 L_s$ is widely employed in the literature [28, 41] and thus feasible to discuss various material models of L_s .

In [1, 42, 43] as well as subsequent work we find

$$i^{\text{BV}} = i_0^{\text{BV}} \cdot \left(e^{\alpha \cdot \frac{e_0}{k_B T} (\eta - E^{(0)}(\bar{y}_A))} - e^{-(1-\alpha) \cdot \frac{e_0}{k_B T} (\eta - E^{(0)}(\bar{y}_A))} \right) \quad (169)$$

with $\eta = \Phi_1 - \Phi_2$, where Φ_2 is “is measured with a lithium reference electrode” [1, p.1527] and Φ_1 the electrostatic potential in the active phase. For the exchange current density i_0^{BV} we find various models:

■ In [42] we find

$$i_0^{\text{BV}} = k \cdot (1 - y_{\text{A}}|_{\text{AE}})^{(1-\alpha)} (y_{\text{A}}|_{\text{AE}})^\alpha \quad \text{with } k = \text{const.} \quad (170)$$

■ In [42] we find

$$i_0^{\text{BV}} = k \cdot (1 - y_{\text{A}}|_{\text{AE}})^{(1-\alpha)} (y_{\text{A}}|_{\text{AE}})^\alpha (1 - y_{\text{E}}|_{\text{AE}})^{(1-\alpha)} (y_{\text{E}}|_{\text{AE}})^\alpha \quad \text{with } k = \text{const.} \quad (171)$$

■ In [35, 44] we find

$$i_0^{\text{BV}} = k \cdot (1 - y_{\text{A}}|_{\text{AE}})^{(1-\alpha)} (y_{\text{A}}|_{\text{AE}})^\alpha (y_{\text{E}}|_{\text{AE}})^\alpha \quad \text{with } k = \text{const.} \quad (172)$$

This model for the Butler–Volmer-reaction rate became a standard in the literature of modeling intercalation batteries [45–49] and is implemented in various software packaged to simulate battery cycles (*i.e.* COMSOL[®], Battery Design Studio[50], BEST [35, 44]) as well as a basis for the interpretation of experimental data[51].

We compare the Butler–Volmer equation (169) to the surface reaction rate (168) and discuss the thermodynamic consistency of the three models (170) - (172) for the exchange current density. Latz *et. al* [52], Bazant [21], and Dreyer *et. al*[26] also point out the importance of thermodynamic consistency of the Butler–Volmer-equation to achieve some overall predictive model since it couples the different thermodynamic bulk models.

First of all we mention again that the Butler–Volmer-equation (168) is derived from surface thermodynamics (see section 2.4) and that the exchange current density $e_0 L_s$ is the Onsager coefficient of the surface reaction 2.7. This yields some necessary constraints on L_s in terms of the functional dependency on the concentrations (or mole fractions) evaluated at the interface $\Sigma_{\text{A,E}}$, which are discussed in 2.7.

By comparison of eq. (168) and (169) we obtain

$$\Phi_1 = \varphi|_{\text{AE}}^- \quad \text{and} \quad \Phi_2 = \varphi|_{\text{AE}}^+ + \frac{k_{\text{B}}T}{E_0} f_{\text{E}}(y_{\text{E}}|_{\text{AE}}), \quad (173)$$

which somehow For a metallic lithium counter electrode, where the reaction



is in thermodynamic equilibrium we have (45) entails

$$\varphi|_{x=x_{\text{EC}}}^- = \varphi|_{x=x_{\text{EC}}}^+ \frac{1}{e_0} (\mu_{\text{C}_C} - g_{\text{A}_C}^R - \kappa_{\text{E}} g_{\text{E}_S}^R) - \frac{k_{\text{B}}T}{e_0} f_{\text{E}}(y_{\text{E}_C}|_{\text{EC}}) \quad (175)$$

which somehow justifies the interpretation of Φ_2 as the potential “is measured with a lithium reference electrode” [1, p.1527]. However, from a thermodynamic point of view this *re-definition* of the potential is not necessary and could lead to inconsistencies when not applied in all balance equations (*e.g.* of the electrolyte transport) and boundary conditions of the intercalation battery model.

For the exchange current density $e_0 L_s$ we showed in section 2.7 that if L_s is dependent on the concentrations at the interface $\Sigma_{\text{A,E}}$, the dependency is for the electrolyte species is necessarily

$$L_s = L_{\text{E}} \left(\mu_{\text{E}_C}(y_{\text{E}_C}|_{\text{AE}}^+) - e_0 U_{\text{E}}^{\text{SCL}} \right) = \hat{L}_{\text{E}} \left(y_{\text{E}_C}|_{\text{AE}}^+ \cdot e^{-\frac{e_0}{k_{\text{B}}T} U_{\text{E}}^{\text{SCL}}} \right). \quad (176)$$

and for the intercalated ions in the active phase

$$L_s = L_s^A(\mu_{A_C}(y_{A_C}|_{AE})) = \hat{L}_s^A(y_{A_C}|_{AE}), \quad (177)$$

or overall

$$L_s = \hat{L}_s(y_{E_C}|_{AE}^+ \cdot e^{-\frac{e_0}{k_B T} U_E^{SCL}}, y_{A_C}|_{AE}). \quad (178)$$

with $U_{AE}^{DL} = \varphi|_{AE}^- - \varphi|_{AE}^+$. Comparing these constraints with the models of the exchange current densities (170) – (170) clearly shows that the dependency of i_0^{BV} on the mole fraction $y_{E_C}|_{AE}^+$ (or concentration $n_{E_C}|_{AE}^+$) of the electrolyte concentration is not compatible with a reaction rate based on non-equilibrium surface thermodynamics. The concentration dependence is already embedded in the term $f_E(y_{E_C}|_{AE})$ of the surface affinity λ_s (164). A dependency of the exchange current density on $y_A|_{AE}$ is in principle compatible with surface thermodynamics. All three models propose

$$i_0^{BV} \propto (1 - y_A|_{AE})^{(1-\alpha)} (y_A|_{AE})^\alpha \quad (179)$$

which in terms of the surface Onsager coefficient would be

$$L_s^A = L_s \cdot (1 - y_A|_{AE})^{(1-\alpha)} (y_A|_{AE})^\alpha \quad \text{and} \quad L_s = \text{const.} > 0. \quad (180)$$

In order to discuss the validity, predictability and finally the necessity (or non-necessity) of a concentration dependent surface Onsager coefficient L_s^A (or exchange current density), we pursue the same strategy and scalings as in section 3, however, now with the model (180). We compute the cell voltage E as function of the capacity Q/Q_A^V and the C-rate C_h in the hierarchy of approximations **BV 1** – **BV 5** and compare it to the computations based on the constant Onsager coefficient.

Eq. (51) reduces with negligible double layer contributions to

$$i = -e_0 L_s \cdot (1 - y_A|_{AE})^{(1-\alpha)} (y_A|_{AE})^\alpha \cdot g\left(\frac{1}{k_B T} \lambda\right). \quad (181)$$

We consider again the scaling

$$e_0 L_s = \tilde{L} \cdot i_A^C = \tilde{L} \frac{d_A \cdot q_A^V}{1 [\text{h}]}. \quad (182)$$

which yields the cell voltage

$$E = E_{A,C} - \frac{k_B T}{e_0} (f_A - f_E|_{AE} + f_E|_{EC}) - g^{-1}\left(-\frac{\frac{C_h}{L}}{(1 - y_A|_{AE})^{(1-\alpha)} (y_A|_{AE})^\alpha}\right) - U_A^{\text{bulk}} + U_E^{\text{bulk}}. \quad (183)$$

Consider the approximation of infinite conductivity in both phases as well as infinite fast diffusion in the electrolyte, *i.e.* the approximation **BV 3**. Fig. 16 shows computations of cell voltage with constant exchange current density as well as concentration dependent exchange current density, for slow ($\tilde{D}_A = 1$) and fast ($\tilde{D}_A = 10$) diffusion in the active particle phase.

The impact of the model (180) for the Onsager coefficient (or the exchange current density) on the cell voltage is surprisingly small. Quite similar to the assumed concentration independence of the diffusion coefficients D_A and D_E we can conclude that $L_s = \text{const.}$ is a rather

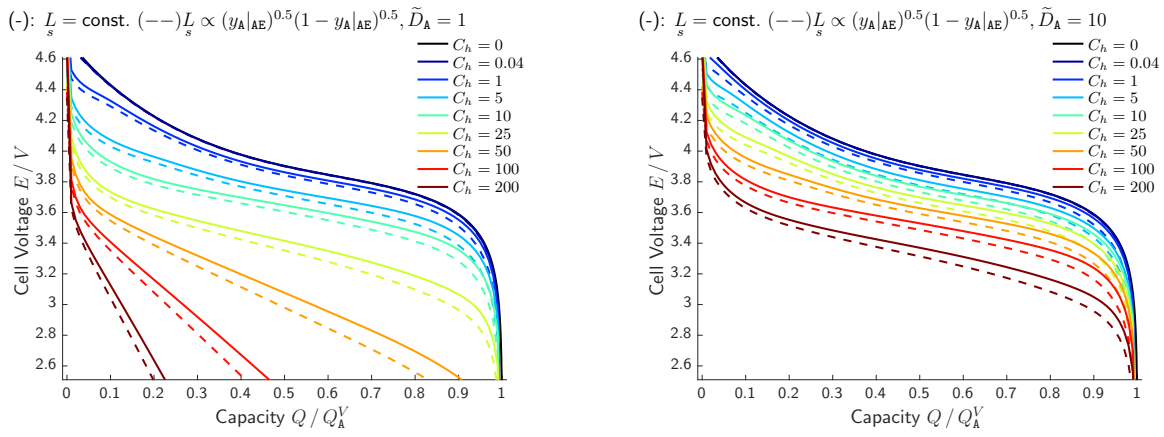


Figure 16: Comparison of the compute cell voltage for the exchange current density according to eq. (180) (–) and a constant surface Onsager coefficient $L_s = \text{const.}$ for various C-rates and slow diffusion (left) as well as fast diffusion (right).

good approximation for the overall modeling procedure. However, well defined and reproduce experimental data sets to compute absolute and relative model errors are rare throughout the literature and the deviations in 16 within the experimental variability. We conclude hence that the model (180) is in principle thermodynamically consistent, when embedded rigorously as stated in section 2, however, a constant exchange current density produces also very reasonable results and is thus the first choice.

4.3 Summary

In this work we discuss the cell voltage E of a non-porous intercalation half-cell during galvanostatic discharge with a continuum model for the active intercalation phase, the adjacent electrolyte, and boundary conditions coupling the phases. Based on non-equilibrium surface thermodynamics a reaction rate for the intercalation reaction $\text{Li}^+ + e^- \rightleftharpoons \text{Li}$ is stated and the measured cell voltage E subsequently derived. We emphasize some necessary restrictions on the exchange current density of the surface reaction rate in terms of concentration dependence to ensure surface thermodynamic consistency.

For the detailed investigation of the non-equilibrium processes, scalings of all non-equilibrium parameters, *i.e.* the diffusion coefficients D_A and D_E of the active phase and the electrolyte, conductivity σ_A and σ_E of both phases, and the exchange current density $e_0 L_s$ of the intercalation reaction, with respect to the 1-C current density i_A^C are introduced. The current density i , entering the model via the boundary conditions, is then expressed as multiple of i_A^C , *i.e.* $i = C_h \cdot i_A^C$, where C_h is the C-rate. Further we derive an expression for the capacity Q of the intercalation cell, which allows us to compute numerically the cell voltage E as function of the capacity Q for various C-rates C_h . Within a hierarchy of approximations, *e.g.* open circuit potential, infinite conductivity, infinite fast diffusion, and so forth, we provide simulations of $E = E(C_h, Q)$ for various values of the (non-dimensional) parameters $(\tilde{\sigma}_A, \tilde{\sigma}_E, \tilde{D}_A, \tilde{D}_E, \tilde{L})$, scaled with respect to the material constant i_A^C . This provides an overall view of the processes and scalings within a lithium ion half cell which is validated at experimental data of $\text{Li}_x(\text{Ni}_{1/3}\text{Mn}_{1/3}\text{Co}_{1/3}\text{O}_2(\text{NMC}))$.

References

- [1] M. Doyle, T. Fuller, J. Newman, *J. Electrochem. Soc.*, 1993, **140**, 1526–1533.
- [2] S.-L. Wu, W. Zhang, X. Song, A. K. Shukla, G. Liu, V. Battaglia, V. Srinivasan, *J. Electrochem. Soc.*, 2012, **159**, A438–A444.
- [3] J. Newman, *Trans. Faraday Soc.*, 1965, **61**, 2229–2237.
- [4] M. Landstorfer, *J. Electrochem. Soc.*, 2017, **164**, E3671–E3685.
- [5] W. Dreyer, C. Guhlke, R. Muller, *Phys. Chem. Chem. Phys.*, 2015, **40**, 27176–27194.
- [6] I. Müller, *Thermodynamics*, Pitman, 1985.
- [7] S. de Groot, P. Mazur, *Non-Equilibrium Thermodynamics*, Dover Publications, 1984.
- [8] W. Dreyer, C. Guhlke, R. Müller, *WIAS Preprint 2511*, 2018.
- [9] M. Landstorfer, C. Guhlke, W. Dreyer, *Electrochim. Acta*, 2016, **201**, 187 – 219.
- [10] W. Dreyer, C. Guhlke, M. Landstorfer, *Electrochem. Commun.*, 2014, **43**, 75 – 78.
- [11] W. Dreyer, C. Guhlke, R. Muller, *Phys. Chem. Chem. Phys.*, 2013, **15**, 7075–7086.
- [12] M. Landstorfer, *Electrochem. Commun.*, 2018, **92**, 56 – 59.
- [13] W. Dreyer, C. Guhlke, M. Landstorfer, R. Müller, *Eur. J. Appl. Math.*, 2018, **29**, 708–753.
- [14] J. W. Cahn, J. E. Hilliard, *J. Chem. Phys.*, 1958, **28**, 258–267.
- [15] J. W. Cahn, *J. Chem. Phys.*, 1959, **30**, 1121–1124.
- [16] R. Garcia, C. Bishop, W. Carter, *Acta Mater.*, 2004, **52**, 11–21.
- [17] W. Dreyer, M. Gaberescek, C. Guhlke, R. Huth and J. Jamnik, *Eur. J. Appl. Math.*, 2011, **22**, 267–290.
- [18] W. Dreyer, C. Guhlke, R. Huth, *Physica D*, 2011, **240**, 1008 – 1019.
- [19] M. Landstorfer, S. Funken, T. Jacob, *Phys. Chem. Chem. Phys.*, 2011, **13**, 12817–12825.
- [20] M. Landstorfer, T. Jacob, *Chem. Soc. Rev.*, 2013, **42**, 3234–3252.
- [21] M. Z. Bazant, *Acc. Chem. Res.*, 2013, **46**, 1144–1160.
- [22] O. Redlich, A. T. Kister, *Ind. Eng. Chem.*, 1948, **40**, 345–348.
- [23] D. K. Karthikeyan, G. Sikha, R. E. White, *J. Power Sources*, 2008, **185**, 1398 – 1407.
- [24] M. Landstorfer, *WIAS Preprint 2560*, 2018.
- [25] A. Sommerfeld, H. Bethe, in *Aufbau der zusammenhängenden Materie*, Springer, 1933, pp. 333–622.
- [26] W. Dreyer, C. Guhlke, R. Muller, *Phys. Chem. Chem. Phys.*, 2016, **18**, 24966–24983.

- [27] J. Newman, T. Chapman, *AIChE Journal*, 1973, **19**, 343–348.
- [28] J. Newman, K. Thomas, *Electrochemical Systems*, John Wiley & Sons, 2014.
- [29] R. M. Fuoss, *J. Solution Chem.*, 1978, **7**, 771–782.
- [30] R. M. Fuoss, L. Onsager, *J. Phys. Chem.*, 1957, **61**, 668–682.
- [31] J. Liu, C. W. Monroe, *Electrochim. Acta*, 2014, **135**, 447 – 460.
- [32] J. Newman, D. Bennion, C. W. Tobias, *Berichte der Bunsengesellschaft für physikalische Chemie*, 1965, **69**, 608–612.
- [33] A. Sanfeld, *Introduction to the thermodynamics of charged and polarized layers*, Wiley, 1968.
- [34] S. U. Kim, V. Srinivasan, *J. Electrochem. Soc.*, 2016, **163**, A2977–A2980.
- [35] A. Latz, J. Zausch, *J. Power Sources*, 2011, **196**, 3296–3302.
- [36] A. Sanfeld, A. Passerone, E. Ricci, J. Joud, *Surf. Sci. Lett.*, 1989, **219**, L521 – L526.
- [37] R. Defay, I. Prigogine, A. Sanfeld, *J. Colloid Interface Sci.*, 1977, **58**, 498 – 510.
- [38] K. A. Jarvis, Z. Deng, L. F. Allard, A. Manthiram, P. J. Ferreira, *Chem. Mater.*, 2011, **23**, 3614–3621.
- [39] K. Shaju, P. Bruce, *Adv. Mater.*, 2006, **18**, 2330–2334.
- [40] N. Nitta, F. Wu, J. T. Lee, G. Yushin, *Mater. Today*, 2015, **18**, 252 – 264.
- [41] A. J. Bard, L. R. Faulkner, *Electrochemical methods: fundamentals and applications*, Wiley New York, 1980, vol. 2.
- [42] T. Fuller, M. Doyle, J. Newman, *J. Electrochem. Soc.*, 1994, **141**, 1–9.
- [43] R. Darling, J. Newman, *J. Electrochem. Soc.*, 1997, **144**, 4201–4208.
- [44] G. B. Less, J. H. Seo, S. Han, A. M. Sastry, J. Zausch, A. Latz, S. Schmidt, C. Wieser, D. Kehrwald, S. Fell, *J. Electrochem. Soc.*, 2012, **159**, A697–A704.
- [45] M. Doyle, J. Newman, A. Gozdz, C. Schmutz, *J. Electrochem. Soc.*, 1996, **143**, 1890–1903.
- [46] Q. Zhang, Q. Guo, R. White, *J. Electrochem. Soc.*, 2006, **153**, A301.
- [47] A. Latz, J. Zausch, O. Iliev, in *Numerical Methods and Applications*, ed. I. Dimov, S. Dimova and N. Kolkovska, Springer Berlin / Heidelberg, 2011, vol. 6046 of Lecture Notes in Computer Science, pp. 329–337.
- [48] W. Lai, F. Ciucci, *Electrochim. Acta*, 2011, **56**, 4369 – 4377.
- [49] A. Jokar, B. Rajabloo, M. Désilets, M. Lacroix, *J. Power Sources*, 2016, **327**, 44 – 55.
- [50] R. Spotnitz, *Battery Design Studio* (<http://www.batdesign.com/>).

[51] P.-C. Tsai, B. Wen, M. Wolfman, M.-J. Choe, M. S. Pan, L. Su, K. Thornton, J. Cabana, Y.-M. Chiang, *Energy Environ. Sci.*, 2018, **11**, 860–871.

[52] A. Latz, J. Zausch, *Electrochim. Acta*, 2013, **110**, 358 – 362.

Appendices

A Electrolyte

A.1 Mole fractions

We consider complete dissociation of the electrolyte and can thus express the mole fractions y_α in terms of n_E , *i.e.*

$$y_{EC} = \frac{n_{EC}}{n} = \frac{n_E}{n_{ES}^R + \left(2 - \frac{(v_{EA} + v_{EC})}{v_{ES}}\right)n_E} \quad (184)$$

$$y_{ES} = \frac{n_{ES}}{n} = \frac{n_{ES}^R - \frac{(v_{EA} + v_{EC})}{v_{ES}}n_E}{n_{ES}^R + \left(2 - \frac{(v_{EA} + v_{EC})}{v_{ES}}\right)n_E}, \quad (185)$$

and $y_{EA} = y_{EC}$ according to the electroneutrality condition. Note we assume

$$v_{EA}^R = v_{EC}^R = \kappa_E v_{ES}^R \quad (186)$$

whereby

$$y_{EC} = \frac{n_{EC}}{n} = \frac{n_E}{n_{ES}^R + 2(1 - \kappa_E)n_E} \quad (187)$$

$$y_{ES} = \frac{n_{ES}}{n} = \frac{n_{ES}^R - 2\kappa_E n_E}{n_{ES}^R + 2(1 - \kappa_E)n_E}. \quad (188)$$

We can also express y_α as function of n_E , *i.e.*

$$y_{EC} = \frac{n_E}{n_E^{\text{tot}}} = \frac{n_E}{n_{ES}^R - 2\kappa_E n_E} \quad (189)$$

A.2 Thermodynamic factor

$$\Gamma_E^{\text{tf}} = \frac{y_{EC}}{k_B T} \frac{\partial \hat{\mu}_{EC}}{\partial y_{EC}} = 1 + 2\kappa_E \frac{y_E}{1 - 2y_{EC}} = \Gamma_E^{\text{tf}}(y_E). \quad (190)$$

Further

$$n_{EC} = y_{EC} \cdot n = n_{ES}^R \frac{y_{EC}}{1 + 2(\kappa_E - 1)y_E} = n_{EC}(y_E). \quad (191)$$

whereby

$$\frac{\partial n_E}{\partial y_E} = n_{E_S}^R \frac{1 + 2(\kappa_E - 1)y_E - y_E^2(\kappa_E - 1)}{(1 + 2(\kappa_E - 1)y_E)^2} = n_{E_S}^R \frac{1}{(1 + 2(\kappa_E - 1)y_E)^2} \quad (192)$$

and thus

$$h_E(y_E) = \frac{1}{n_E^R} \frac{\partial n_E}{\partial y_E} = \frac{n_{E_S}^R}{n_E^R} \frac{1}{(1 + 2(\kappa_E - 1)y_E)^2} =: \cdot \quad (193)$$

Finally we have also

$$\tilde{c}_E^{\text{tot},R}(y_E) = \frac{n_E^{\text{tot}}}{n_E^R} = \frac{n_{E_S}^R}{n_E^R} \cdot \frac{1}{1 + 2(\kappa_E - 1)y_E} \quad (194)$$

A.3 PDEPE syntax for the electrolyte phase

We want to solve numerically the problem

$$\tilde{d} \cdot \tilde{q}^V \cdot \tilde{t}_E \frac{C_h}{D_E} h_E(y_E) \frac{\partial y_E}{\partial \tau} = \partial_\xi (s_E^{\text{tot}}(y_E) \Gamma_E^{\text{tf}}(y_E) \cdot \partial_\xi y_E) \quad (195)$$

with boundary conditions

$$\left(\tilde{c}_E^{\text{tot},R} \Gamma_E^{\text{tf}} \partial_\xi y_E \right) \Big|_{\xi=0} = \frac{C_h}{D_E} \quad \text{and} \quad \left(\tilde{c}_E^{\text{tot},R} \Gamma_E^{\text{tf}} \partial_\xi y_E \right) \Big|_{\xi=1} = \frac{C_h}{D_E} \quad (196)$$

and

$$h_E(y_E) = \frac{n_{E_S}^R}{n_E^R} \frac{1}{(1 + 2(\kappa_E - 1)y_E)^2} \quad (197)$$

$$\Gamma_E^{\text{tf}}(y_E) = 1 + 2\kappa_E \frac{y_E}{1 - 2y_{E_C}} \quad (198)$$

$$\tilde{c}_E^{\text{tot},R} = \frac{n_{E_S}^R}{n_E^R} \frac{1}{1 + 2(\kappa_E - 1)y_E} \quad (199)$$

Note that it is ever convenient for the numerical computation of $y_E \in (0, 0.5)$ to introduce the variable

$$u = \frac{1}{a} \ln \left(\frac{2y_E}{1 - 2y_E} \right) = \hat{u}(2y_E) \quad (200)$$

which yields

$$y_E = \frac{1}{2} \cdot \frac{e^{au}}{1 + e^{au}} = \frac{1}{2} \hat{y}(u) \quad (201)$$

The parameter a can be adjusted for numerical computations.

Correspondingly, we obtain

$$h_E(y_E) = h_E\left(\frac{1}{2}\hat{y}(u)\right) \quad (202)$$

$$\Gamma_E^{\text{tf}}(y_E) = \Gamma_E^{\text{tf}}\left(\frac{1}{2}\hat{y}(u)\right) \quad (203)$$

$$\tilde{c}_E^{\text{tot},R}(y_E) = \tilde{c}_E^{\text{tot},R}\left(\frac{1}{2}\hat{y}(u)\right) \quad (204)$$

and

$$\partial_\tau y_E = \frac{1}{2} \partial_u \hat{y} \cdot \partial_\tau u, \quad \partial_x y_E = \frac{1}{2} \partial_u \hat{y} \cdot \partial_x u \quad (205)$$

with

$$\partial_u \hat{y} = \frac{ae^{au}(1+e^u) - ae^u e^u}{(1+e^{au})^2} = a \frac{e^{au}}{(1+e^{au})^2} =: g_u(u) \quad (206)$$

This yields

$$\tilde{p} \cdot \frac{C_h}{D_E} h_E \left(\frac{1}{2} \hat{y}(u) \right) \frac{1}{2} g_u(u) \frac{\partial u}{\partial \tau} = \partial_\xi \left(\tilde{c}_E^{\text{tot},R} \left(\frac{1}{2} \hat{y}(u) \right) \Gamma_E^{\text{tf}} \left(\frac{1}{2} \hat{y}(u) \right) \frac{1}{2} g_u(u) \cdot \partial_\xi u \right) \quad (207)$$

with boundary conditions

$$\left(\tilde{c}_E^{\text{tot},R} \left(\frac{1}{2} \hat{y}(u) \right) \Gamma_E^{\text{tf}} \left(\frac{1}{2} \hat{y}(u) \right) \frac{1}{2} g_u(u) \cdot \partial_\xi u \right) \Big|_{\xi=0} = \frac{C_h}{D_E} \quad (208)$$

$$\left(\tilde{c}_E^{\text{tot},R} \left(\frac{1}{2} \hat{y}(u) \right) \Gamma_E^{\text{tf}} \left(\frac{1}{2} \hat{y}(u) \right) \frac{1}{2} g_u(u) \cdot \partial_\xi u \right) \Big|_{\xi=1} = \frac{C_h}{D_E} \quad (209)$$

and

$$\tilde{p} := \tilde{d} \cdot \tilde{q}^V \cdot \tilde{t}_E \quad (210)$$

The initial value is

$$y_E(x, t = 0) = y_E(\bar{n}_E) \quad (211)$$

and transfers as

$$u(x, t = 0) = \hat{u}(2y_E(\bar{n}_E)). \quad (212)$$

PDEPE takes the form

$$c(u) \partial_\tau u + \partial_\xi (f(u, \partial_\xi u)) = 0 \quad (213)$$

with boundary conditions

$$p_l(u|_{x=x_l}) + q_l \cdot f(u, \partial_\xi u) \Big|_{x=x_l} = 0 \quad \text{and} \quad p_r(u|_{x=x_r}) + q_r \cdot f(u, \partial_\xi u) \Big|_{x=x_r} = 0. \quad (214)$$

We have hence

$$c = \tilde{p} \cdot \frac{C_h}{D_E} h_E \left(\frac{1}{2} \hat{y}(u) \right) \frac{1}{2} g_u(u) \quad (215)$$

$$f = \tilde{c}_E^{\text{tot},R} \left(\frac{1}{2} \hat{y}(u) \right) \Gamma_E^{\text{tf}} \left(\frac{1}{2} \hat{y}(u) \right) \frac{1}{2} g_u(u) \cdot \partial_\xi u \quad (216)$$

and

$$p_l = \frac{C_h}{D_E} \quad p_r = \frac{C_h}{D_E} \quad (217)$$

$$q_l = -1 \quad q_r = -1 \quad (218)$$

B Active particle

B.1 Thermodynamic factor

We consider for the chemical potential in the active particle phase

$$\mu_A = k_B T \left(\ln \left(\frac{\frac{1}{\omega_A} y_A}{1 + \frac{1-\omega_A}{\omega_A} y_A} \right) - \omega \cdot \ln \left(\frac{1-y_A}{1 + \frac{1-\omega_A}{\omega_A} y_A} \right) + \gamma_A \cdot g_A(y_A) \right) \quad (219)$$

with

$$g(y) = (2y-1) + \frac{1}{2}(6y(1-y) - 1) - \frac{1}{3}(8y(1-y) - 1)(2y-1) \quad (220)$$

Hence

$$\frac{\partial \mu_A}{\partial y_A} = \frac{1}{y_A (1-y_A) \left(\frac{1}{\omega_A} y_A + (1-y_A) \right)} + \gamma_A \cdot \partial_y g \quad (221)$$

with

$$\partial_y g = 16 \cdot y^2 - 22y_A + \frac{25}{3}. \quad (222)$$

The thermodynamic factor Γ_A^{tf} is then

$$\Gamma_A^{\text{tf}} = y_A \cdot \frac{\partial f_A}{\partial y_A} = \frac{1}{(1-y_A) \left(\frac{1}{\omega_A} y_A + (1-y_A) \right)} + \gamma_A \cdot \left(16 \cdot y_A^3 - 22y_A^2 + \frac{25}{3} y_A \right). \quad (223)$$

B.2 PDEPE notation

We seek to solve (109), *i.e.*

$$\frac{C_h}{\overline{D_A}} \frac{\partial y_A}{\partial \tau} = \partial_\xi \left(y_A \frac{\partial f_A}{\partial y_A} \partial_\xi y_A \right) \quad (224)$$

with boundary conditions (110)

$$y_A \frac{\partial f_A}{\partial y_A} \partial_\xi y_A \Big|_{\xi=0} = 0 \quad \text{and} \quad y_A \frac{\partial f_A}{\partial y_A} \partial_\xi y_A \Big|_{\xi=1} = \frac{C_h}{\overline{D_A}}. \quad (225)$$

and

$$y_A \frac{\partial f_A}{\partial y_A} = \Gamma_A^{\text{tf}} = y_A \cdot \frac{\partial f_A}{\partial y_A} = \frac{1}{(1-y_A) \left(\frac{1}{\omega_A} y_A + (1-y_A) \right)} + \gamma_A \cdot \left(16 \cdot y_A^3 - 22y_A^2 + \frac{25}{3} y_A \right). \quad (226)$$

Note that it is ever convenient for the numerical computation of $y_A \in (0, 1)$ to introduce the variable

$$u = \ln \left(\frac{y_A}{1-y_A} \right) \quad (227)$$

which yields

$$y_A = \frac{e^u}{1 + e^u} \quad (228)$$

We have hence

$$\partial_\tau y_A = \partial_u y_A \cdot \partial_\tau u \quad (229)$$

and

$$\partial_x y_A = \partial_u y_A \cdot \partial_x u \quad (230)$$

with

$$\partial_u y_A = \frac{e^u (1 + e^u) - e^u e^u}{(1 + e^u)^2} = \frac{e^u}{(1 + e^u)^2} =: g(u) \quad (231)$$

PDEPE takes the form

$$c(u) \partial_\tau u + \partial_\xi (f(u, \partial_\xi u)) = 0 \quad (232)$$

with boundary conditions

$$p_l(u|_{x=x_l}) + q_l \cdot f(u, \partial_\xi u)|_{x=x_l} = 0 \quad \text{and} \quad p_r(u|_{x=x_r}) + q_r \cdot f(u, \partial_\xi u)|_{x=x_r} = 0. \quad (233)$$

We have hence

$$c = \frac{C_h}{\widetilde{D_E}} g_u(u) \quad (234)$$

$$f = \Gamma_A^{\text{tf}}(\hat{y}_A(u)) g_u(u) \cdot \partial_\xi u \quad (235)$$

and

$$p_l = 0 \quad p_r = \frac{C_h}{\widetilde{D_E}} \quad (236)$$

$$q_l = 1 \quad q_r = -1 \quad (237)$$

Note that we introduce the *stop-event* $y_A|_{AE} < 1 - 10^{-10}$ for the time-integration of pdepe.